

KARMA



Karst Aquifer Resources availability and quality in the **Mediterranean Area**

Uncertainties in water budget

Deliverable 2.7

Authors:

Marco Petitta (URO), Valeria Lorenzi (URO), Marino Domenico Barberio (URO), Chiara Sbarbati (URO), Mohamed Al Ali (AUB), Bartolomé Andreo Navarro (UMA), Juan Antonio Barberá Fornell (UMA), Rachida Boulilla (ENIT), Guillaume Cinkus (UMO), Emma Gargouri-Ellouze (ENIT), Joanna Doummar (AUB), Jaime Fernández Ortega (UMA), Nico Goldscheider (KIT), Hervé Jourde (UMO), José Francisco Martín Rodríguez (UMA), Naomi Mazzilli (UMO), Jihad Othman (AUB) and Fairouz Slama (ENIT).

Date: March 2022



This project has received funding from the European Union's PRIMA research and innovation programme



Project Partners



(Coordinator)



SAPIENZA
UNIVERSITÀ DI ROMA



Executive Summary

WP2 deals with the evaluation of water availability at the five test sites in KARMA project using different methods. The previous deliverables consisted of a preliminary assessment (D2.1 Preliminary water budget) of the water balance (recharge/discharge) in individual test sites, using available data and (recent and historical) information. Thus, a first estimation of karst groundwater resources was established.

A subsequent deliverable (D2.2 Recharge evaluation) comprised the core activity of the Task 2.1 “Recharge assessment and tracer tests”, and it includes an updated estimation of recharge rates in the KARMA test sites. The final goal is to provide a distributed recharge map for the studied areas at a catchment scale in a continental Mediterranean context. Therefore, a more accurate recharge assessment was performed in each study area, as described in the following chapters.

The common research approach in D2.2 consisted of the application of the APLIS method, originally developed by members of the UMA partner (Andreo et al., 2008; Marin, 2009). The application of APLIS at different test sites different from the climatic and hydrogeological contexts in which the method was originally designed also serves as a test of its robustness and reliability.

In following steps, provided results on the spatial distribution of aquifer recharge have been compared with discharge measurements for the investigated karst systems (D2.6 Spring Discharge Monitoring). Besides APLIS, alternative approaches (i.e. hydraulic modeling, stable isotopes – see D2.3, tracer tests – see D2.4) have been performed in some individual test sites for the same purpose.

In the present deliverable, the results obtained for aquifer recharge of each study area are discussed in terms of their reliability to evaluate the intrinsic uncertainty, which can be due to the lack and gap in recharge evaluation, as in discharge measurements. The adopted methods for validating the water budget proposed in D2.2 allow each research group to limit the uncertainties, towards a final comparison of the obtained results. It emerges from collected data that water budget validation and limitation of uncertainties can be obtained by different approaches in karst systems. Some methods appear as feasible in each test study, some others can be adapted and considered useful also in areas where they have been not applied. Nevertheless, it also is clear that the karst behavior and the consequent hydrogeological setting of groundwater flow is influencing the recharge/discharge conditions, making some method easier to apply in specific conditions, with respect to other methods which are more useful in a general context. Finally, the aquifer extension and the scale of observations have an influence in favoring the adoption of a method or another one in validating the water budget.

A final further step for WP2 will be the comparison of the results obtained for water budget in each study area, to possibly evaluate: i) a potential common impact/trend in groundwater resource availability and renewal rate in different study areas (climate change effects); ii) a best-practice proposal for improving the water budget calculation in karst aquifers in Mediterranean area.

Table of contents

1 Introduction	3
2 Gran Sasso aquifer (Case Study Italy).....	4
2.1 General description of the test site	4
2.2 Methodology	5
2.3 Results.....	5
2.4 Water Budget Validation	18
2.5 Conclusions.....	23
2.6 References	24
3 The Djebel Zaghouan aquifer (Case Study Tunisia).....	25
3.1 Study Area.....	25
3.2 Water Budget Summary	26
3.3. Weakness and uncertainties of the adopted methods	30
3.4. Conclusion	32
3.5 References	32
4 The Qachqouch aquifer (Case Study Lebanon)	33
4.1 Study Area: The Qachqouch spring.....	33
4.2 Water Budget Result Summary	33
4.3 Weakness and uncertainties of the adopted methods	35
4.4 Conclusion	37
4.5 References	37
5 Eastern Ronda Mountains and Ubrique test site (case study Spain)	38
5.1 Introduction.....	38
5.2 Water Budget Summary	39
5.3 Weakness and Uncertainties of the adopted methods	41
5.4 Validation Tools	42
5.5 Discussion and Conclusions	43
5.6 References	44
6 The Lez Karst Catchment (case study France).....	46
6.1 Water Budget Results Summary	46
6.2 Weakness and uncertainties of the adopted methods	46
6.3 Validation Tools	51
6.4 Discussion and Conclusion.....	52
6.5 References	52
7 Conclusions	54

1 Introduction

The overarching objective of the KARMA project is to achieve substantial progress in the hydrogeological understanding and sustainable management of karst groundwater resources in the Mediterranean area in terms of water availability and quality. At karst catchment scale, the main objective is to advance and compare transferable modeling tools for improved predictions of climate-change impacts and better-informed water management decisions, and to prepare vulnerability maps as tools for groundwater quality protection.

The main objective of WP2 is the assessment of groundwater availability by investigating recharge, discharge and storage. Recharge consists of the downward flow of rainwater that reaches the water table. Recharge into karst and fissured aquifers can occur in two ways, (1) diffusely over carbonate outcrops, epikarst and soils (autogenic) or (2) from nearby non-karst areas where rainwater infiltrates through swallow holes or dolines (allogenic) (Figure 1.1).

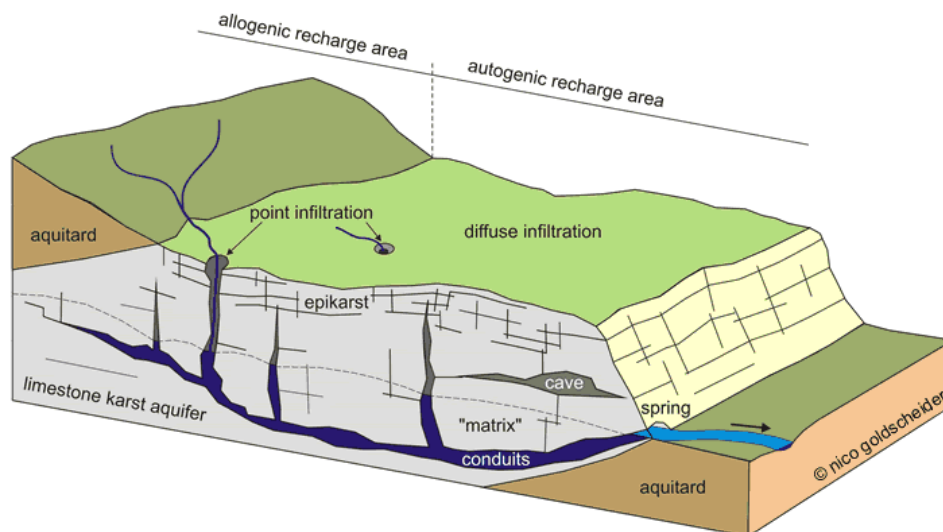


Figure 1.1. Schematic illustration of a heterogeneous karst aquifer system characterized by a duality of recharge (allogenic vs. autogenic), infiltration (point vs. diffuse) and porosity/flow (conduits vs. matrix) (Goldscheider 2019)

The available knowledge about these processes and how infiltration takes place in each KARMA test site highly influences the development of numerical models and vulnerability maps, as well as their accuracy. Therefore, in order to achieve a better hydrogeological understanding and to obtain reliable data for the calibration and validation of models and vulnerability maps, hydrological monitoring, isotope studies, and tracer tests will be carried out in addition to the recharge rate estimation.

When considering an appropriate time scale (decades), it can be assumed that the mean annual value of the recharge is equivalent to the rate of discharge. Thus, groundwater recharge over a defined area is usually equivalent to infiltration excess. Different methods are traditionally applied for groundwater recharge assessment (i.e. hydrological or numerical balance, based on hydrochemistry and environmental isotopes, etc), however none of them are free from uncertainty. The following chapters will show the results obtained by each research unit in their study area in calculating the water budget, focusing on their uncertainties and the related validation process.

2 Gran Sasso aquifer (Case Study Italy)

2.1 General description of the test site

The Gran Sasso hydrostructure is defined as a calcareous-karstic aquifer system of about 1034 km² of total extension and it can be considered one of the most representative karst aquifers of the central-southern Apennines. The Gran Sasso hydrogeological system, characterised by Meso-Cenozoic carbonate units, is bounded by terrigenous units represented by Miocene flysch (regional aquiclude) along its northern side and Quaternary continental deposits (regional aquitard) along its southern side (Figure 1). The aquifer can be divided into hydrogeological complexes each determined by a specific lithology, porosity and permeability. The Gran Sasso karst regional aquifer fed springs located at the boundary of the system (Figure 2.1). Main springs have been classified into six groups based on groundwater flow and hydrogeochemical characteristics with a total discharge between 18 m³/s and 25 m³/s (Amoruso et al., 2012, Petitta and Tallini, 2002), including a highway tunnel drainage tapped for drinking purpose on both sides, with a net infiltration of about 800 mm/y (Petitta and Tallini, 2002). The aquifer is characterised by an endorheic basin having a tectonic-karst origin, called Campo Imperatore basin (elevation 1650 m a.s.l), that acts as a preferential recharge area, fed by high rainfall and snowfall.

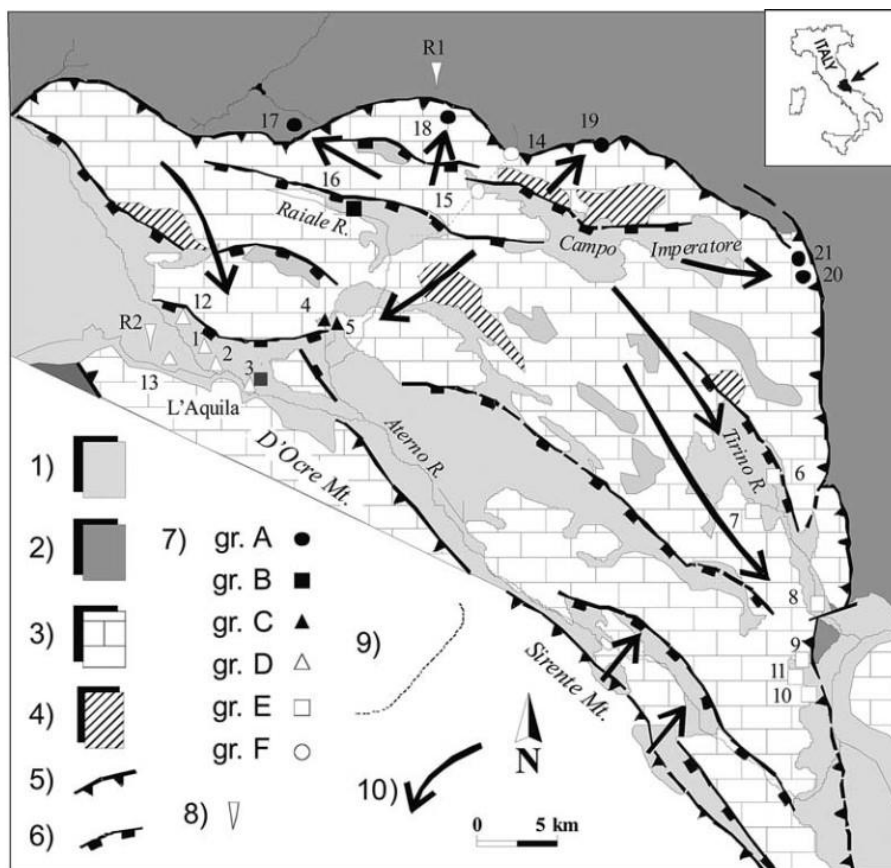


Figure 2.1- Gran Sasso hydrogeological outline. 1: aquitard (continental detrital units of intramontane basins, Quaternary); 2: aquiclude (terrigenous turbidites, Mio-Pliocene); 3: aquifer (calcareous sequences of platform Meso-Cenozoic); 4: low permeability substratum (dolomite, upper Triassic); 5: thrust; 6: extensional fault; 7: main spring: AS: Assergi drainage; RU: Ruzzo drainage; VA: Vacelliera spring; TS: Tirino springs; symbols refer to the six spring groups identified in Barbieri et al. (2005); 8: linear spring; 9: springs belonging to a nearby aquifer; 10: INFN underground laboratories (UL in the text); 11: meteorological station (IS: Isola Gran Sasso, CC: Carapelle Calvisio); 12: presumed water table in m asl; 13: main groundwater flow path; 14: highway tunnels drainage. (Amoruso, 2012)

This report describes an updated assessment of the Gran Sasso water budget obtained through three different methods: Apls (Andreo et al., 2008), Turc (Turc, 1954), and Thornthwaite (Thornthwaite et al., 1957). The aim of this report is the evaluation of the uncertainties of water budget obtained through Thornthwaite method. The validation was carried out by stable isotopic approach and by calculated discharge rates.

2.2 Methodology

To verify the recharge values obtained from the water budget, different validation procedures should be applied. Tracer tests represent the best validation approach (see Deliverable 2.4). For the Gran Sasso aquifer a pilot tracer test will be carried out in March-April 2022. Another validation method consists in the application of lumped parameter model (Deliverable 4.2, Mazzilli et al., 2019, Sivelle et al. 2021). To validate our calculated water budget, we considered the stable isotope results. In particular, the purpose is to compare the $\delta^{18}\text{O}$ values derived from recharge (Ir) and discharge (IQ) data, with measured $\delta^{18}\text{O}$ values obtained from stable isotope analyses of sampled groundwater (Im). In order to obtain $\delta^{18}\text{O}$ values derived from recharge (Ir), a recharge model has been developed by calculating the recharge distribution with altitude (classification in altitude ranges and recharge percentage). By the selection of an adequate vertical isotopic gradient for the study area (from Computed Isotopes Recharge Elevation local equations: CIRE), a specific $\delta^{18}\text{O}$ value (Ic) has been assigned to each altitude range of the aquifer. Each Ic value has been weighted with respect to the recharge percentage assigned to the corresponding altitude ranges (%RA). Therefore, the averaged value Ir is obtained by the sum of each Ic multiplied by the corresponding %RA, as shown in Eq. (1):

$$I_r = \sum (I_{c_n} * \%RA_n) / 100 \quad \text{Isotopic } \delta^{18}\text{O} \text{ values calculated from recharge} \quad \text{Eq. (1)}$$

Where:

Ir: $\delta^{18}\text{O}$ weighted isotope from recharge

Ic_n: $\delta^{18}\text{O}$ Isotope calculated from CIRE.

%RA: percentage recharge related to every altitude range.

To obtain $\delta^{18}\text{O}$ values correlated with discharge (IQ), the mean annual discharge values and mean annual $\delta^{18}\text{O}$ values of each considered spring have been considered. The IQ was obtained multiplying the $\delta^{18}\text{O}$ annual spring mean value (from isotopic results, Ia), by annual mean spring discharge (Qs) of each considered spring; the result has been divided by total annual mean spring discharge Q_{tot}, as shown in Eq. (2):

$$I_Q = \sum (I_{a_n} * Q_{s_n}) / Q_{\text{tot}} \quad \text{Isotopic } \delta^{18}\text{O} \text{ values calculated from discharge} \quad \text{Eq. (2)}$$

Where:

I_Q: $\delta^{18}\text{O}$ weighted isotope from discharge

I_{a_n}: $\delta^{18}\text{O}$ average isotope value of springs

Q_{s_n}: average discharge of springs

Q_{Tot}: total discharge, as sum of all Q_{s_n}

2.3 Water Budget summary

This chapter shows the data required to apply the selected method of water budget validation. In detail, the recharge elaboration and the altitude recharge distribution have been calculated by

applying of three different methods: Turc, Thornthwaite, and APLIS (see Deliverable 2.2). In addition, discharge data and stable isotope results are included.

2.3.1 Water budget result summary

The results obtained from the three selected different methods are based on the thermorain gauges shown in Figure 2.2 and used as a starting point for the recharge calculation (see Deliverables 2.2 for details). The same figure 2.2 includes the location of discharge measurement sites used for the validation of the water budget.

Detailed information on water budget calculation is included in D2.2.

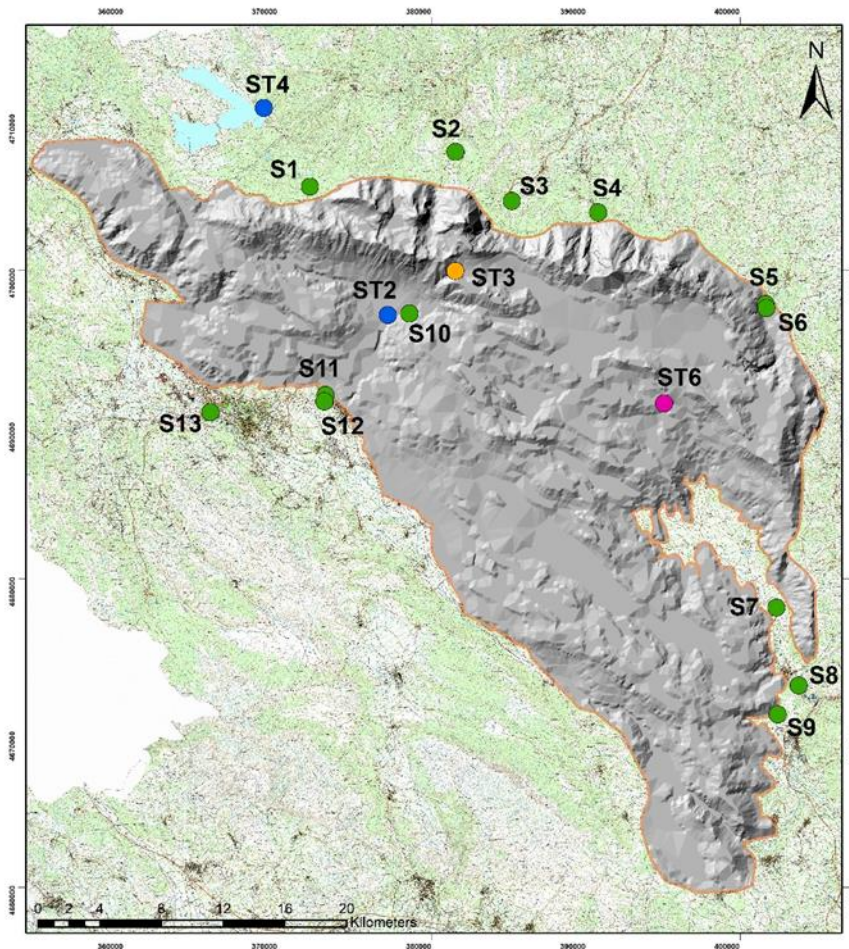


Figure 2.2: Location of thermorain gauges and the main springs of the aquifer. ST2) Assergi thermorain gauges, ST3) Campo Imperatore thermorain and snow gauge, ST4) Campotosto thermorain gauge, ST6) Castel del Monte thermorain gauge. S1-S13) spring locations

As explained in D2.2, by Turc method, the total average recharge value for the 2001-2020 period is $19.9 \text{ m}^3/\text{s}$, with a contribution due to snowmelt of $3.2 \text{ m}^3/\text{s}$. The mean evapotranspiration is $444 \text{ mm}/\text{y}$, while the average infiltration value from rainfall corresponds to $508 \text{ mm}/\text{y}$, added to $98 \text{ mm}/\text{y}$ due to snowmelt. The year 2007 and year 2013 represent the driest and the rainiest year, respectively. In 2007 the calculated recharge corresponds to $11.5 \text{ m}^3/\text{s}$ ($10 \text{ m}^3/\text{s}$ from rainfall and $1.5 \text{ m}^3/\text{s}$ from snowmelt), while in 2013 the total value of recharge reaches $30.7 \text{ m}^3/\text{s}$ (Table 2.1). Figure 2.3 resumes the yearly recharge results obtained by Turc method.

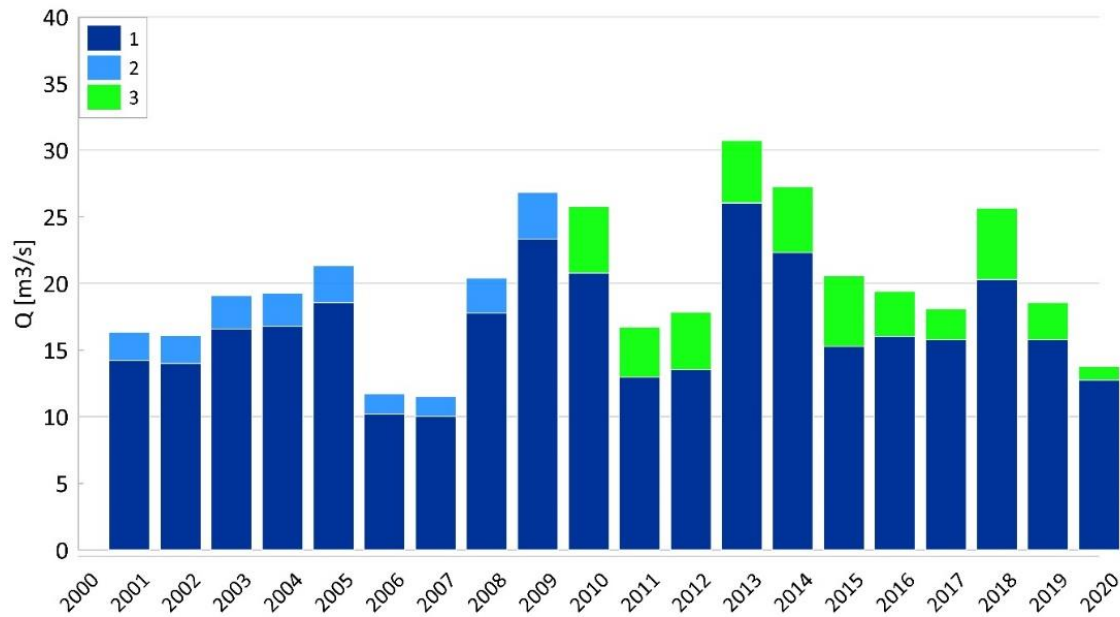


Figure 2.3: Yearly recharge results by Turc application: 1) recharge from rainfall; 2) estimated snow contribution (assumed as 15% of recharge); 3) calculated snow contribution

By Thornthwaite method, a total average recharge for 2001-2020 period of 18.5 m³/s (15.3 m³/s from rainfall and 3.2 m³/s from snowmelt) has been calculated. The real evapotranspiration (ETR) value is 491 mm/y, while the total infiltration value is 558 mm/y, considering the infiltration from rainfall of 462 mm/y and infiltration from the snowmelt of 97 mm/y. Also in this case, the 2013 is confirmed as rainiest year, with a total recharge value of 27.3 m³/s and a total infiltration value of 832 mm/y. On the other hand, as far as the driest year is concerned, this is identified as 2006, with a total recharge value of 9.8 m³/s and with a total infiltration value of 297 mm/y (Table 2.1, Figure 2.4).

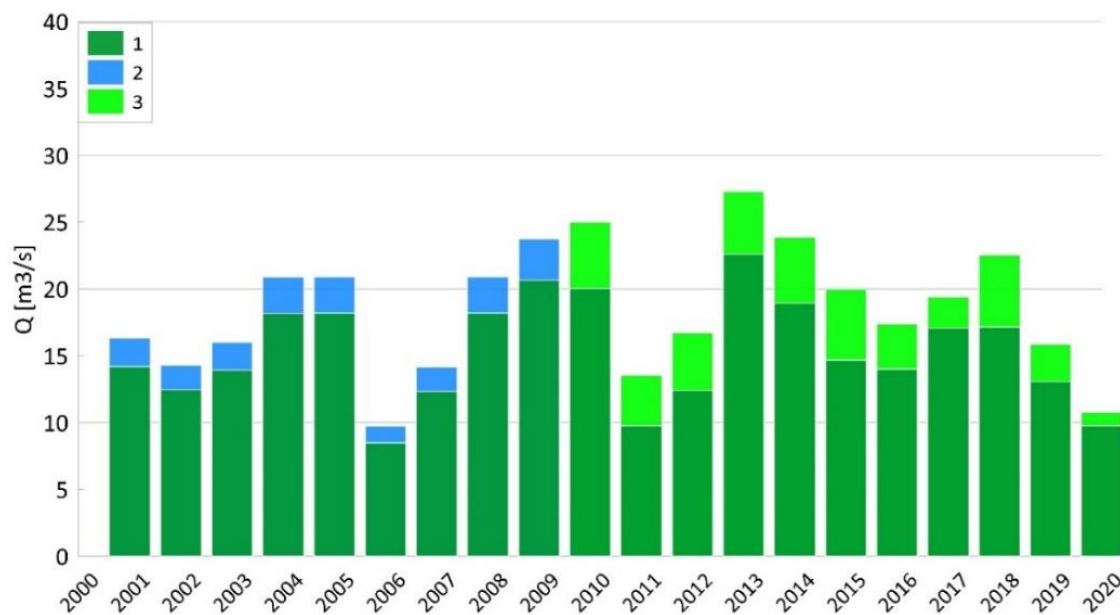


Figure 2.4: Yearly recharge results by Thornthwaite application: 1) recharge from rainfall; 2) estimated snow contribution (assumed as 15% of recharge); 3) calculated snow contribution

Table 2.1: The water budget parameters and the average recharge for period 2001-2020 obtained by Turc and Thornthwaite methods. In addition, the years with the maximum and minimum recharge values are also shown.

Turc	Mean	Driest year	Rainiest year
	2001-2020	2007	2013
P [mm]	955	701	1255
T [°C]	9.8	9.9	9.6
ETR [mm]	444	393	458
R [mm]	3	2	4
I rainfall [mm]	508	305	794
I snow [mm]	98	46	143
I total [mm]	606	351	937
Q rainfall [m³/s]	16.7	10	26
Q snow [m³/s]	3.2	1.5	4.7
Q tot [m³/s]	19.9	11.5	30.7

Thornthwaite	Mean	Driest year	Rainiest year
	2001-2020	2006	2013
P [mm]	955	703	1255
T [°C]	9.8	9.4	9.6
ETR [mm]	491	443	562
R [mm]	3	2	4
I rainfall [mm]	462	259	689
I snow [mm]	97	39	143
I total [mm]	558	297	832
Q rainfall [m³/s]	15.3	8.5	22.6
Q snow [m³/s]	3.2	1.3	4.7
Q tot [m³/s]	18.5	9.8	27.3

Through the Aplis method, the Gran Sasso aquifer recharge results in a percentage of effective infiltration of 51.6% with respect to total rainfall. The Gran Sasso massif, according to Aplis, is characterized by a preferential recharge area, the Campo Imperatore basin, with an infiltration rate of 76.7%. (Figure 2.5).

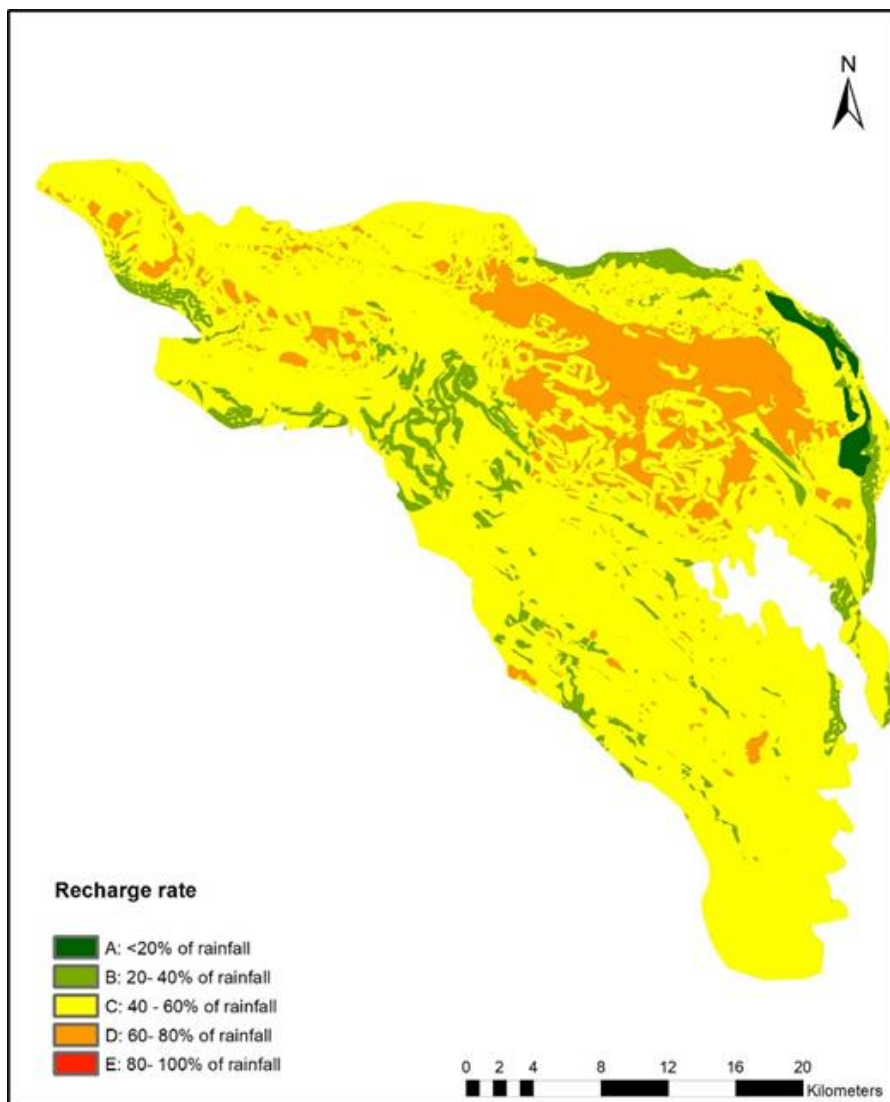


Figure 2.5: Recharge rate map obtained by Aplis method: letters refer to 5 infiltration rate classes

Overlaying the obtained recharge rate map (Figure 2.5) to the raster rainfall map obtained for each year, the yearly aquifer recharge has been obtained (Figure 2.6).

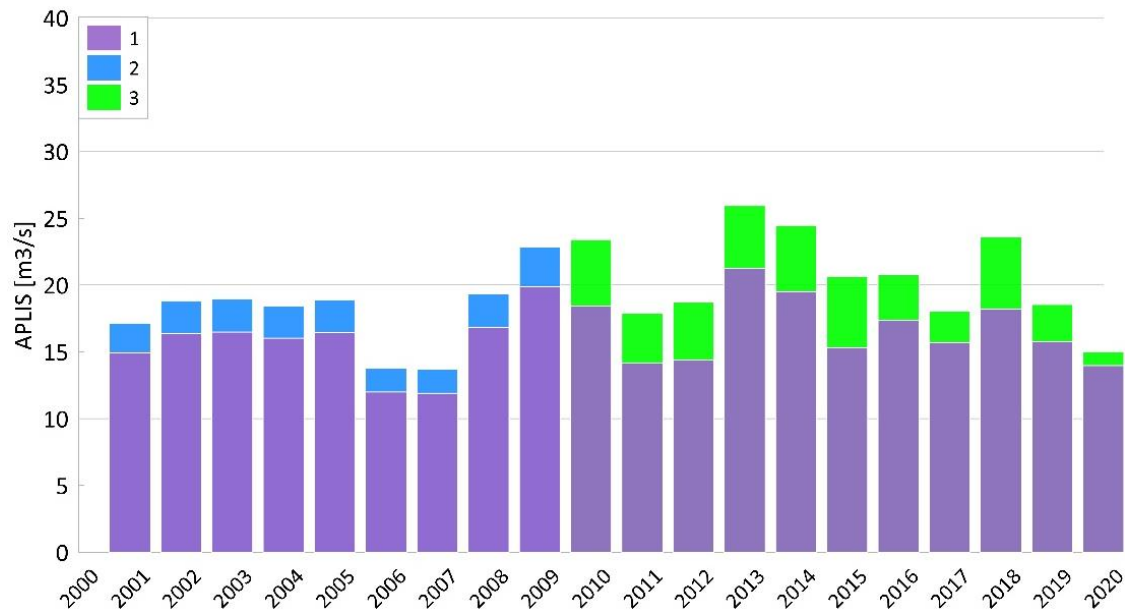


Figure 2.6: Yearly recharge results by Aplis application: 1) recharge from rainfall; 2) estimated snow contribution (assumed as 15% of recharge); 3) calculated snow contribution

The average recharge rate on long-term period is 19.4 m³/s, and the average infiltration is 594 mm/y. The 2007 year represents the year with a minimum recharge rate of 13.7 m³/s, while 2013 is characterised by the highest recharge rate of 21.3 m³/s. In Table 2.2 the infiltration and recharge values of the average, driest and rainiest years are summarised.

Table 2.2: Gran Sasso water budget values obtained by Aplis method

Aplis	Mean	Driest year	Rainiest year
	2001-2020	2007	2013
I rainfall [mm]	496	363	649
I snow [mm]	98	54	143
I total [mm]	594	418	792
Q rainfall [m ³ /s]	16.2	11.9	21.3
Q snow [m ³ /s]	3.2	1.8	4.7
Q tot [m ³ /s]	19.4	13.7	25.9

In Figure 2.7, the long monitoring period (L), the driest (C) and the rainiest (R) years are illustrated for the APLIS method. For the long-term period, the most representative is the “B Class” characterized by an infiltration rate ranging from 20% to 40% (Figure 2.7 L). This category impacts 58% of the whole area, covering the low-altitude areas (< 1000 m), while the remaining 42% is characterized by variable infiltration rates which generally increase according to altitude and reach the maximum at the peak areas (Figure 2.7 L). The driest year is mainly represented by the “A Very Low” class (< 20% of recharge rate), which covers 68% of the recharge area involving the medium-low altitude belts (< 1400 m) (Figure 2.7 C). Differently, in the rainiest year, the “E Very High” class is prevalent (> 80% of recharge rate) covering 32% of the recharge area at the medium-high altitude belts (> 1400 m) (Figure 2.7 R).

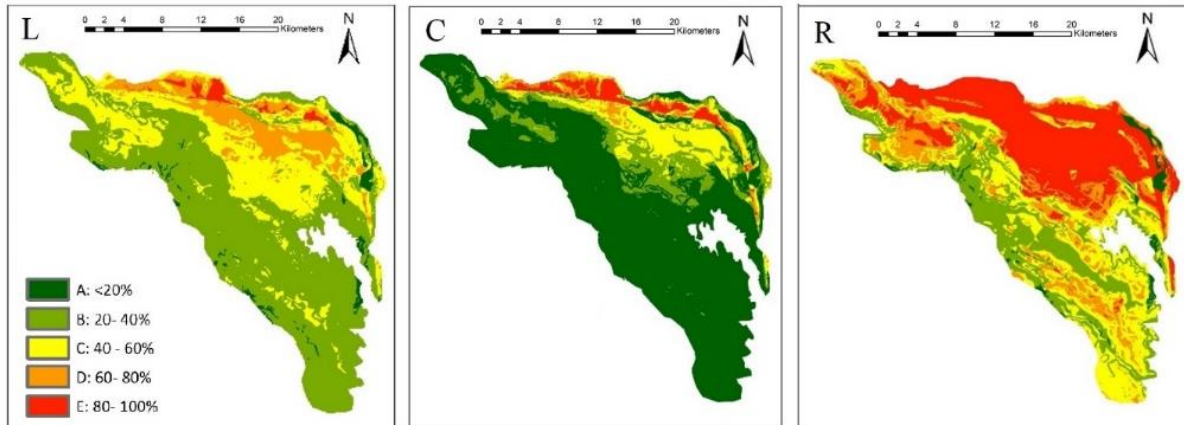


Figure 2.7: Recharge rate distribution calculated by Aplis method for L) long monitoring period; C) the driest year; R) the rainiest year.

The water budget analysis with three different approaches reveals very similar results for each method. In fact, for all methods, the highest recharge value has been recorded in 2013, while the driest years have been recognized in the 2006-2007 period. Rainfall recharge obtained through both methods (Turc and Thornthwaite) over the entire monitoring period has been evaluated in terms of distribution over time and space. The recharge is distributed with elevation based on five different altitude belts (see the ranges in Table 2.3 and Figure 2.8). Specifically, for each altitude belt, recharge values and the corresponding percentage on the total water budget have been calculated (Table 2.3).

Table 2.3: Recharge values calculated with Turc and Thornthwaite methods for each altitude belt for the average, the driest (2006 for Thornthwaite and 2007 for Turc) and the rainiest years (2013).

Altitude range	Area	Year 2000-2020		Driest year				Rainiest year			
		Turc	Thornthwaite	Turc	%	Thornthwaite	%	Turc	%	Thornthwaite	%
<600 m	55 km ²	0.4 m ³ /s	0.3 m ³ /s	0.1 m ³ /s	1	0.1 m ³ /s	1	0.7 m ³ /s	2.5	0.7 m ³ /s	3
600 m – 1000 m	340 km ²	3.6 m ³ /s	2.7 m ³ /s	1.6 m ³ /s	16	1.2 m ³ /s	14	6.1 m ³ /s	23.5	5.1 m ³ /s	23
1000 m – 1400 m	310 km ²	4.9 m ³ /s	4 m ³ /s	3 m ³ /s	30	2.3 m ³ /s	27	7.8 m ³ /s	30	6.5 m ³ /s	29
1400 – 1800 m	227 km ²	4.7 m ³ /s	4 m ³ /s	3.3 m ³ /s	33	2.7 m ³ /s	32	7.0 m ³ /s	27	6.2 m ³ /s	27
>1800	102 km ²	3.1 m ³ /s	3 m ³ /s	2 m ³ /s	20	2.2 m ³ /s	26	4.4 m ³ /s	17	4.1 m ³ /s	18
Total	1034 km²	16.7 m³/s	14 m³/s	10 m³/s	100	8.5 m³/s	100	26 m³/s	100	22.6 m³/s	100

As expected, the minor contribution comes from the lowest altitude belt (< 600 m) with values less or equal to 3% of total recharge in the three analysed conditions. In the 600-1000 m belt, the widest one, the contribution to aquifer recharge increases, showing the widest variation ranging from 14% for the driest year to 23% for the rainiest year (Table 2.3).

In the other altitude ranges (1000-1400 m and 1400-1800 m) there are no significant differences in terms of percentage values of recharge, which vary from 27% to 30% (Table 3). The higher altitude belt (> 1800 m) differently contributes to aquifer recharge, showing the relatively high percentage values in the driest year (Table 3). This evidence points out the fundamental role of the high elevation areas in aquifer recharge, especially in drought periods.

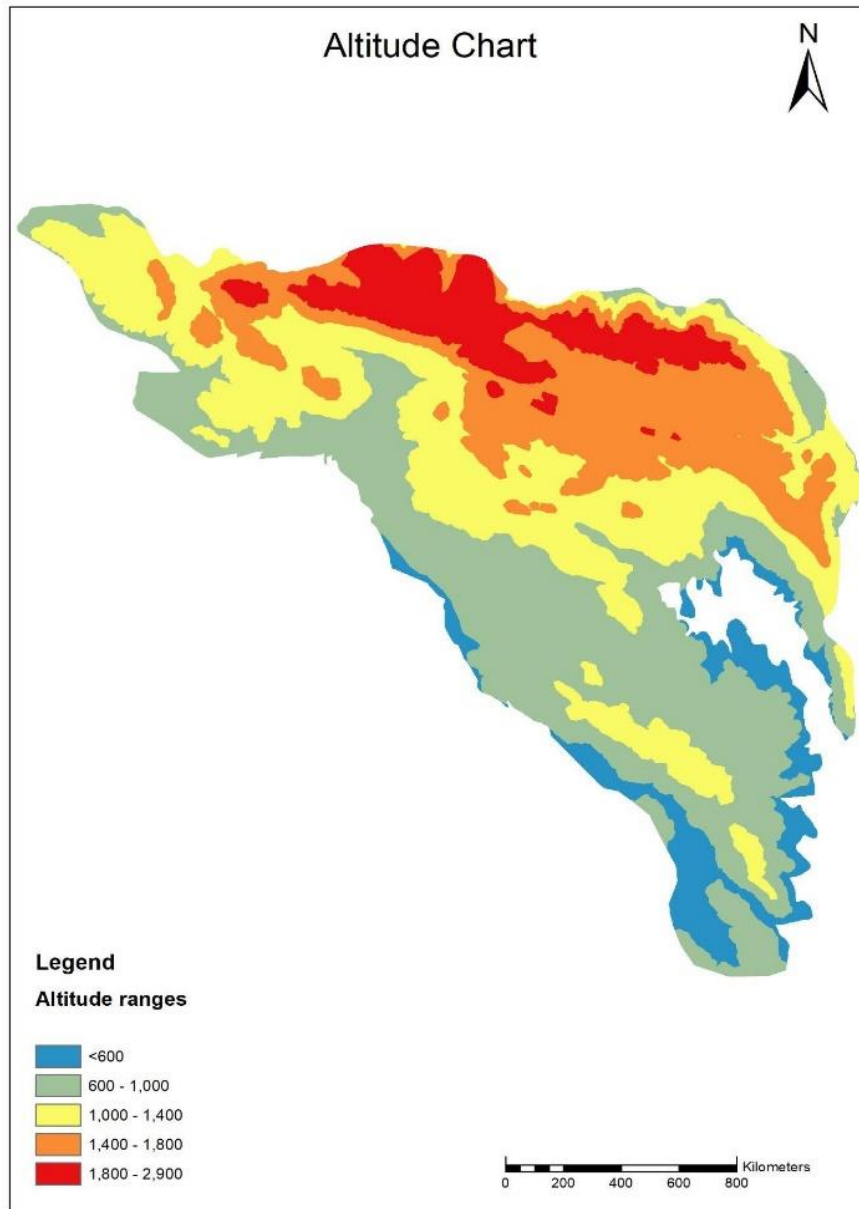


Figure 2.8: Altitude belts for the analyses of rainfall recharge distribution

2.3.2 Discharge

In order to verify the reliability of recharge results obtained with the application of different methods, a comparison with the main springs discharge data over the 2001-2020 period is carried out. The springs that have been considered are listed in Table 4 and their positions are shown in Figure 2. Flow rate data for the monitoring period (2001-2020) are mainly provided by water suppliers and the Regional Environmental Agency. Most of the springs discharge data are unfortunately not continuous for the analysed period. The missing information is therefore derived from the average of the available data or through the correlation line spring flow vs Turc recharge values. The acquired data are checked and validated. The mean discharge value of each spring for the period 2001-2020 is summarised in Table 2.4.

Table 2.4: Mean discharge values (2001-2020) of the selected main springs (see Figure 2.2 for location)

ID	Spring	Mean discharge (2001-2020) [m ³ /s]
S1	Chiarino	0.4
S2	Rio Arno	0.2
S3	Northern Drainage	1.1
S4	Ruzzo	0.8
S5	Vitella d’Oro	0.7
S6	Mortaio d’Angri	0.3
S7	Capodacqua Presciano	5.8
S8	Basso Tirino	6.7
S9	San Calisto	1.4
S10	Southern Drainage	0.5
S11	Tempera	1.2
S12	Vera	0.3
S13	Vetoio-Boschetto	1.0

The total average annual flow rate (in m³/s) from the springs fed by the Gran Sasso aquifer varied between 18 m³/s and 23.7 m³/s. The long-term average flow rate is 20.4 m³/s. The correlation analysis between annual recharge results obtained by the Turc method and the springs discharge, reveals the immediate or time-delayed springs responses with respect to the recharge variations. In detail, most of the spring discharge located on the northern side of the Gran Sasso massif (S1 to S6 in Figure 2.2 and Table 2.4) are marked by fast response to annual recharge. A clear example is represented by the Rio Arno spring (S2 in Figure 2.2). The annual Rio Arno spring discharge (blue dots) follows the yearly variation observed for recharge (orange bars), as shown in Figure 2.9.

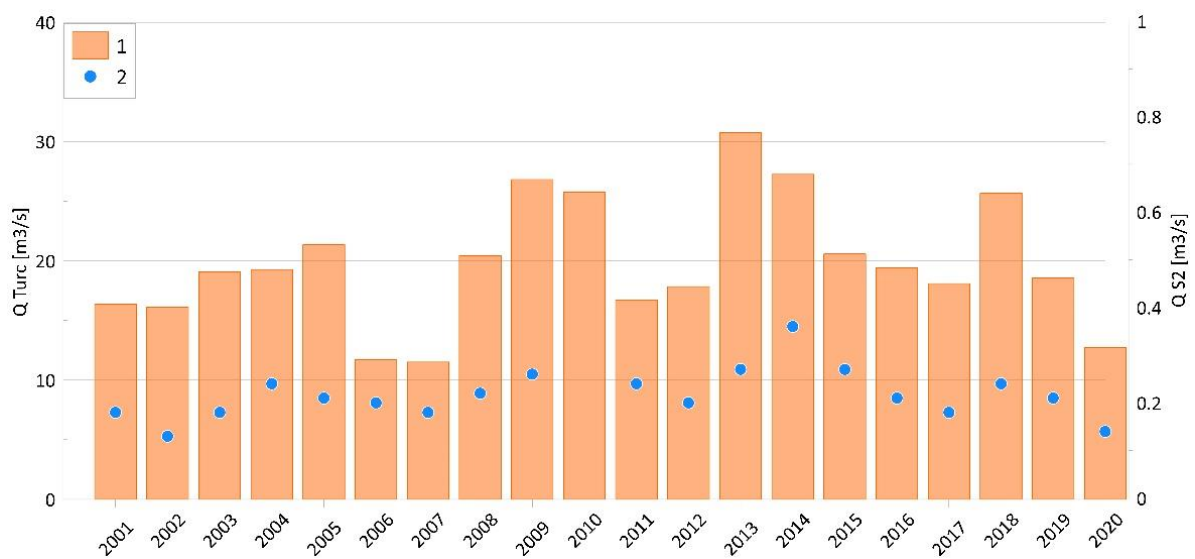


Figure 2.9: Comparison over time between calculated recharge with Turc (1) and Rio Arno (S2 in Figure 2) spring discharge (2); missing dots (2010) correspond to unavailable data.

Conversely, springs monitored on the southern side (S7-S13 in Figure 2.2) reflect the variation in aquifer recharge with some delay. The southern drainage discharge of the highway tunnel, for example, (S10 in Figure 2.2) is correlated with aquifer recharge after one year of delay (Figure 2.10a). The delay is more evident at the Tirino River (S9 in Figure 2.2), whereby the annual Turc value shows its effects approximately by a two years delay (Figure 2.10b).

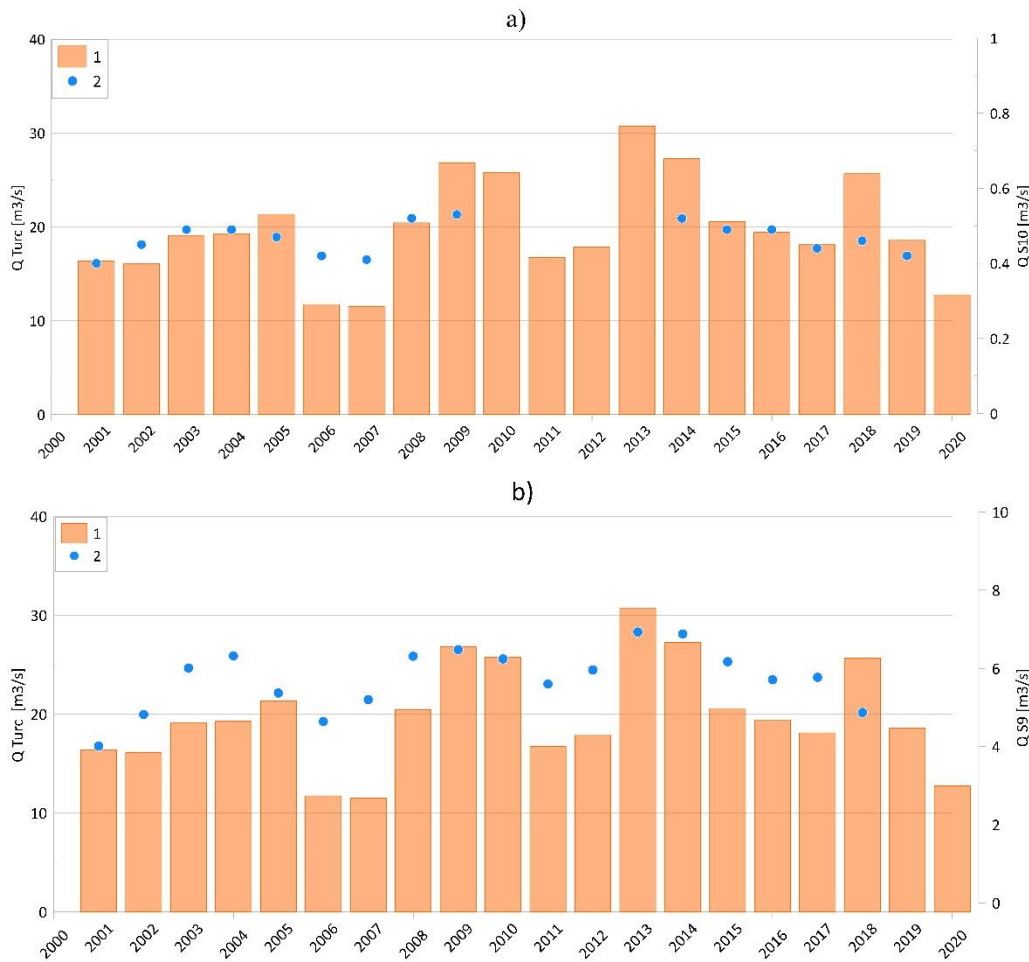


Figure 2.10: Comparison over time between calculated recharge with Turc (1) and spring discharge (2): a) one-year shifted S10 discharge and b) two-year shifted S9 discharge; missing dots mean not available data period

2.3.3 Isotope results

Figure 2.11 shows the location of sampling points of the Gran Sasso monitoring network (springs and groundwater sampled from motorway tunnel). Specifically, the monitoring network consists in 13 main springs (from GS1 to GS14, excluding GS3, GS8 and GS10) and 7 monitoring points representatives of the groundwater collected inside the motorway tunnel (GS3, GS10 and GS15A-B-C-D-E). The numbers correspond to the spring location and are equivalent to the ones numbered in Figure 2.2.

In Table 2.5 and Table 2.6 the stable isotope results of $\delta^{18}\text{O}$ and $\delta^2\text{H}$ of water acquired from previous studies (since 2001 to 2010, Table 2.5) and analysed in KARMA (since 2020 to 2021 Table 2.6) are listed.

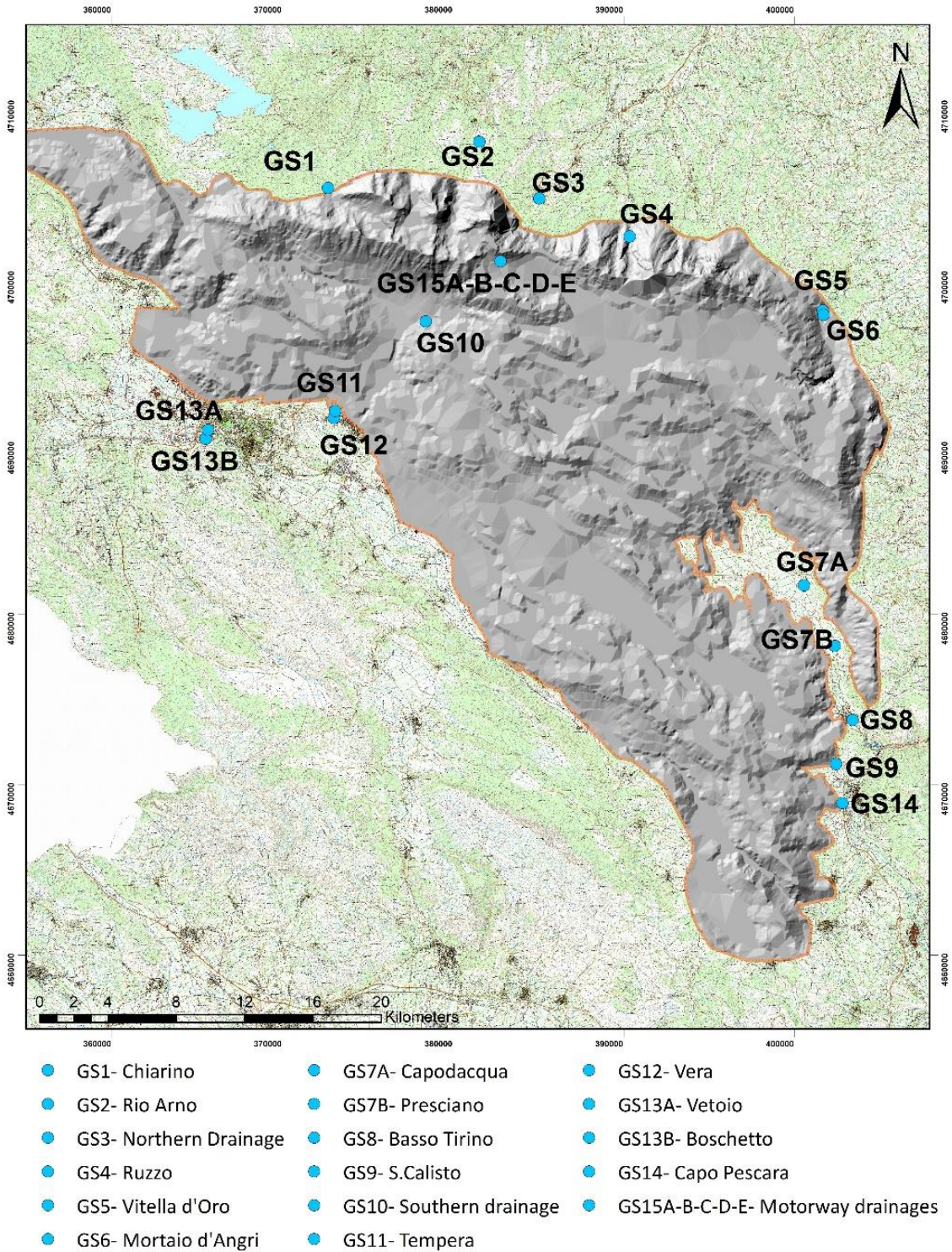


Figure 2.11: Location of isotopically monitored springs.

Table 2.5: Previously collected isotope data. ID refer to Figure 2.11. N.M.= not measured

ID	2001		2006		2007		2010	
	$\delta^2\text{H}$	$\delta^{18}\text{O}$	$\delta^2\text{H}$	$\delta^{18}\text{O}$	$\delta^2\text{H}$	$\delta^{18}\text{O}$	$\delta^2\text{H}$	$\delta^{18}\text{O}$
GS1	-60.4	-9.1	-68.2	-10.3	-70.8	-10.6	-71.7	-10.9
GS2	-67.3	-10.1	-72.9	-10.7	-72.3	-10.9	-68.9	-10.4
GS3	-69.1	-10.1	-74.2	-10.8	-74.7	-11.1	-72.9	-11.1
	-69.5	-10.2	N.M.	N.M.	N.M.	N.M.	N.M.	N.M.
GS4	-65.8	-9.7	-73.0	-10.9	-69.3	-10.7	N.M.	N.M.
GS5	-64.3	-9.7	-70.7	-10.6	-70.9	-10.8	-71.2	-10.6
	N.M.	N.M.	N.M.	N.M.	N.M.	N.M.	-69.8	-10.7
GS6	-66.6	-9.7	-71.3	-10.9	-69.9	-10.7	-69.3	-10.6
	N.M.	N.M.	N.M.	N.M.	N.M.	N.M.	-69.2	-10.6
GS7A	-64.7	-9.7	-69.4	-10.1	-68.8	-10.3	-70.6	-10.2
	-67.7	-10.0	N.M.	N.M.	N.M.	N.M.	-68.4	-10.2
GS7B	-63.5	-9.4	-71.2	-10.3	-69.9	-10.1	-68.6	-10.0
	-66.0	-9.8	N.M.	N.M.	N.M.	N.M.	-68.6	-10.0
GS8	-65.9	-10.0	N.M.	N.M.	N.M.	N.M.	N.M.	N.M.
	-67.6	-10.0	N.M.	N.M.	N.M.	N.M.	N.M.	N.M.
GS9	-64.6	-9.8	-68.5	-9.8	-67.3	-10.1	-68.2	-9.9
	-64.6	-9.8	N.M.	N.M.	N.M.	N.M.	-67.8	-10.0
GS10	-72.91	-10.45	-73.5	-11.0	N.M.	N.M.	N.M.	N.M.
	-75.70	-11.05	N.M.	N.M.	N.M.	N.M.	N.M.	N.M.
GS11	-69.3	-10.2	-71.3	-10.5	-72.7	-10.8	-72.3	-10.7
	-72.3	-10.6	N.M.	N.M.	N.M.	N.M.	-72.7	-10.8
GS12	-69.3	-10.4	-71.7	-10.6	-72.6	-10.8	-71.4	-10.5
	-72.4	-10.6	N.M.	N.M.	N.M.	N.M.	-71.0	-10.5
GS13A	-59.8	-9.1	-63.8	-9.4	-63.8	-9.5	-66.7	-9.6
	N.M.	N.M.	N.M.	N.M.	N.M.	N.M.	-64.7	-9.6
GS13B	-60.7	-9.0	N.M.	N.M.	N.M.	N.M.	N.M.	N.M.
	-63.3	-9.4	N.M.	N.M.	N.M.	N.M.	N.M.	N.M.
GS14	-65.5	-9.6	-67.3	-10.0	-69.2	-10.2	-69.0	-10.2
	-67.6	-10.0	N.M.	N.M.	N.M.	N.M.	-67.4	-10.2
GS15A	-72.9	-10.5	N.M.	N.M.	N.M.	N.M.	N.M.	N.M.

In Figure 2.12 the isotope results are displayed with respect to local meteoric water lines as listed below:

$$\delta\text{D}\text{‰} = 7.7 \delta^{18}\text{O} + 9.8 \quad (\text{Eq. 3 Barbieri et al., 2003})$$

$$\delta\text{D}\text{‰} = 7.76 \delta^{18}\text{O} + 9.95 \quad (\text{Eq. 4 Barbieri et al., 2005})$$

$$\delta\text{D}\text{‰} = 7.047 \delta^{18}\text{O} + 5.608 \quad (\text{Eq. 5 Longinelli and Selmo, 2003})$$

$$\delta\text{D}\text{‰} = 7.62 \delta^{18}\text{O} + 12.5 \quad (\text{Eq. 6 Celico et al., 1984})$$

Table 2.6: KARMA isotope data. ID refer to Figure 2.11.

2020				2021			
ID	Date	$\delta^2\text{H}$	$\delta^{18}\text{O}$	ID	Date	$\delta^2\text{H}$	$\delta^{18}\text{O}$
GS1	28/10/2020	-69.6	-10.8	GS1	19/05/2021	-65.0	-10.1
GS2	28/10/2020	-69.3	-10.6	GS1	05/07/2021	-61.9	-10.4
GS3	28/10/2020	-73.7	-11.3	GS1	31/08/2021	-67.5	-10.4
GS5	27/10/2020	-70.2	-10.7	GS2	19/05/2021	-66.5	-10.2
GS6	27/10/2020	-69.7	-10.8	GS2	05/07/2021	-67.5	-10.3
GS7A	23/10/2020	-67.9	-10.4	GS2	31/08/2021	-67.8	-10.6
GS7B	23/10/2020	-66.8	-10.2	GS3	01/03/2021	-69.6	-10.8
GS10	28/10/2020	-71.9	-11.0	GS3	17/06/2021	-72.6	-11.1
GS11	27/10/2020	-70.9	-11.0	GS3	30/08/2021	-67.6	-10.3
GS12	27/10/2020	-69.3	-10.6	GS4	17/06/2021	-65.7	-10.3
GS13A	27/10/2020	-59.3	-9.1	GS5	01/03/2021	-65.3	-10.2
GS13B	27/10/2020	-63.1	-9.6	GS5	28/04/2021	-65.0	-10.2
GS15A	28/10/2020	-73.4	-11.2	GS5	23/06/2021	-67.0	-10.5
GS15B	28/10/2020	-73.1	-11.2	GS5	30/08/2021	-67.6	-10.6
GS15C	28/10/2020	-73.0	-11.1	GS6	01/03/2021	-67.3	-10.5
GS15D	28/10/2020	-72.7	-11.1	GS6	23/06/2021	-67.5	-10.5
GS15E	28/10/2020	-71.3	-11.0	GS6	30/08/2021	-68.2	-10.6
				GS7B	02/03/2021	-65.3	-9.9
				GS7B	13/07/2021	-66.4	-10.0
				GS7B	08/09/2021	-67.0	-10.5
				GS9	08/09/2021	-70.3	-10.7
				GS10	06/07/2021	-72.4	-11.1
				GS11	02/03/2021	-69.2	-10.6
				GS11	18/06/2021	-71.4	-10.8
				GS11	30/08/2021	-69.1	-10.6
				GS12	02/03/2021	-70.3	-10.6
				GS12	30/08/2021	-71.1	-10.7
				GS12	18/06/2021	-70.9	-10.8
				GS13A	02/03/2021	-61.1	-9.2
				GS13A	18/06/2021	-61.9	-9.3
				GS13A	30/08/2021	-67.0	-10.3
				GS13B	02/03/2021	-62.1	-9.4
				GS13B	17/06/2021	-61.9	-9.3
				GS13B	30/08/2021	-67.7	-10.5
				GS14	02/03/2021	-65.9	-10.1
				GS14	08/09/2021	-71.9	-11.1
				GS15B	22/07/2021	-73.8	-11.3
				GS15C	22/07/2021	-73.4	-11.2
				GS15D	22/07/2021	-73.6	-11.2
				GS15E	17/06/2021	-71.3	-11.0

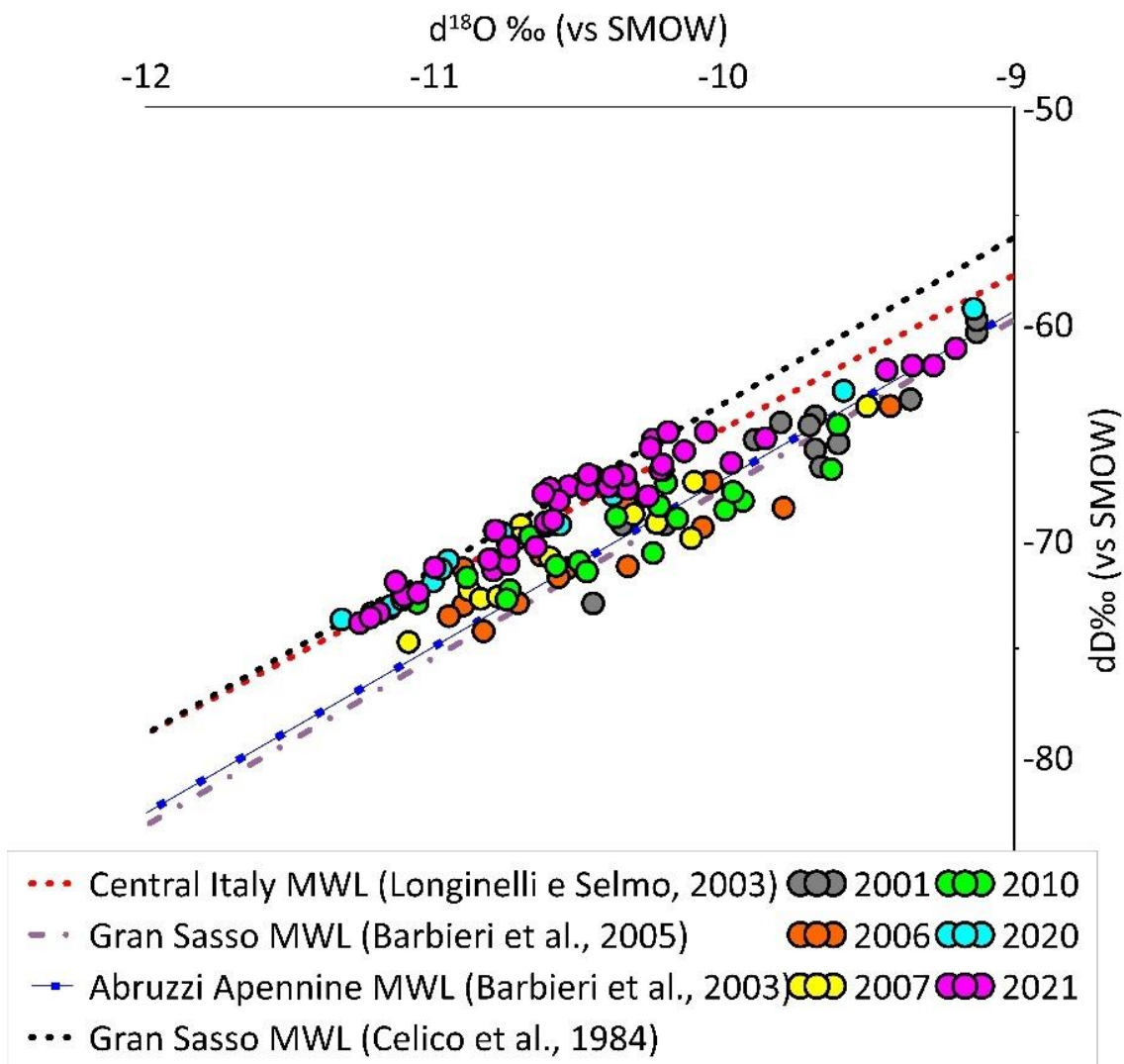


Figure 2.12: Correlation between $\delta^{18}O$ and δ^2H values and meteoric water lines (Barbieri et al., 2003; 2005; Longinelli and Selmo, 2003; Celico et al., 1984)

In Figure 2.12 a good correlation of all data with respect to the available local meteoric water lines is identified. In detail, since 2001 to 2021 the best fitting or real data progressively seems to move from the lowest meteoric water line by Barbieri et al., 2005 to the highest one, proposed by Celico et al., 1984. From these data, specific isotopic vertical gradients have been calculated, and the following equations to assess CIRE (Computed Isotope Recharge Elevation) have been considered. The relationship between $\delta^{18}O$ and altitude is displayed in Figure 2.13:

$$\begin{aligned} \delta^{18}O &= -0.0013h - 8.40 && \text{(Eq. 7 for Abruzzi Apennine, Barbieri et al., 2003)} \\ \delta^{18}O &= -0.0024h - 6.35 && \text{(Eq. 8 for Gran Sasso Aquifer, Barbieri et al., 2005)} \\ \delta^{18}O &= -0.0014h - 7.9315 && \text{(Eq. 9 for Gran Sasso Aquifer, Celico et al., 1984)} \\ \delta^{18}O &= -0.0014h - 5.9054 && \text{(Eq. 10 for Central Italy, Longinelli and Selmo, 2003)} \end{aligned}$$

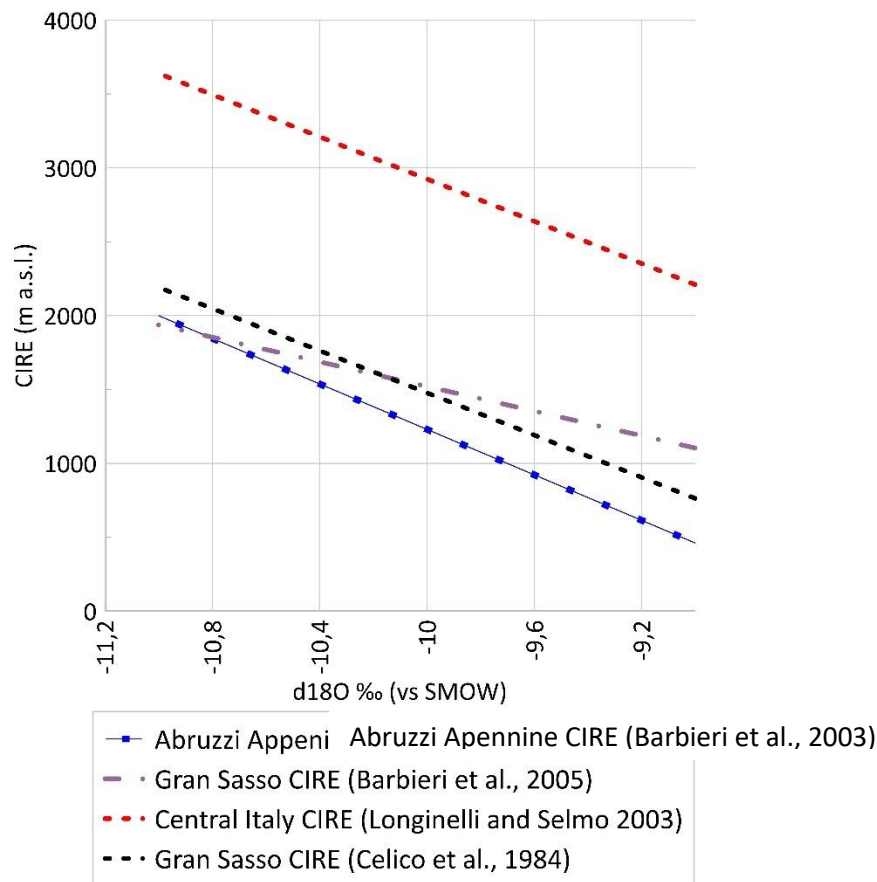


Figure 2.13: Correlation between $\delta^{18}O$ and Altitude (CIRE from Barbieri et al., 2003; 2005; Longinelli and Selmo, 2003; Celico et al., 1984)

2.4 Validation tools

Karst aquifers usually show a fast response to recharge inputs, and consequently, for this study case, a good correlation between recharge and discharge values at the annual scale is expected. In fact, to verify the reliability of the recharge values obtained with the application of different methods, the total spring discharge and recharge values calculated by the above mentioned three different methods have been compared. The major springs considered are shown in Figure 2.2. Figure 2.14 shows the comparison between the annual values of recharge obtained by the three applied methods and the annual measured discharge of the aquifer springs. In detail, the recharge obtained by Thornthwaite method and the total spring discharge (Figure 2.14C) shows a good correlation ($R^2=0.85$). A general underestimation of Thornthwaite recharge with respect to the total spring discharge was observed, which was more evident in the driest years.

On the other hand, Figure 2.14L shows the slight overestimation of Turc recharge with respect to the total spring discharge for the rainy years and a slight underestimation for drought years.

Moreover, the comparison between Aplis and total spring discharge in Figure 2.14R shows the lowest correlation ($R^2=0.81$), confirming a slight underestimation trend of Aplis with respect to total spring discharge. Definitely, adopting the best correlation discharge/recharge and their characteristics, recharge estimation from the Thornthwaite method have been used to validate the calculated water budget.

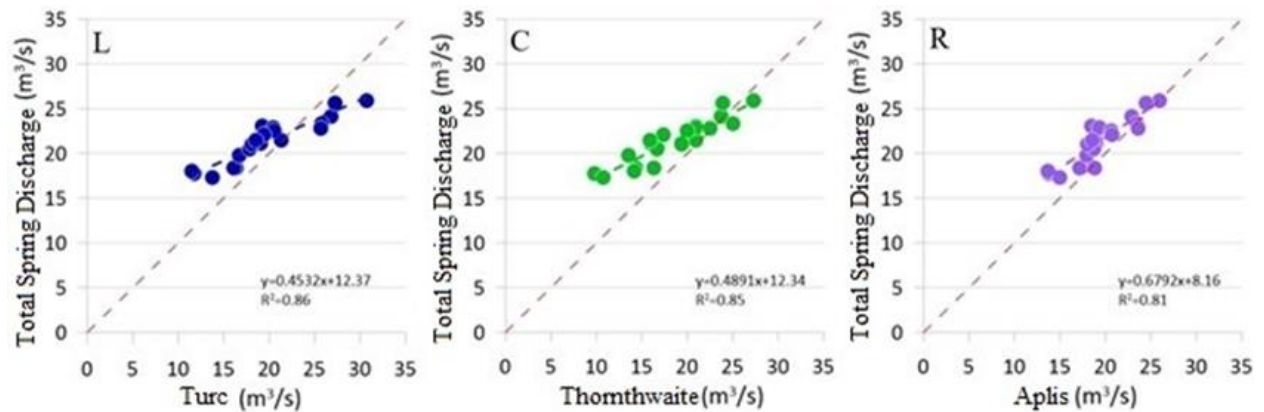


Figure 2.14: Correlation between the yearly recharge calculated in the three different methods (Turc, Thornthwaite and Aplis) and the discharge of the springs considered for each observation year

In order to set up the validation procedure, the weighted isotope calculated from recharge (I_r), the weighted isotope calculated from discharge (I_Q) and measured isotopic values (I_m) have been compared. Due to the limited availability of isotopic data, only 2001, 2006, 2007, 2010, 2020, and 2021 years have been analyzed.

To evaluate weighted isotope values calculated from recharge (I_r), the equation (1) has been applied. The values of single I_c required to calculate I_r ($\delta^{18}O$ values assigned to each altitude range) have been derived both by equation 7 and equation 8, while %RA (recharge percentage related to each altitude range) refer to Thornthwaite method results, as resumed in Table 2.7. Finally, the sum of $I_c \cdot \%RA$ corresponding to I_r has been obtained.

To evaluate weighted isotope values from discharge (I_Q), the equation (2) has been applied. The I_a ($\delta^{18}O$ annual average values) and Q_s (discharge annual average values) have been calculated only for springs where both data are available, as shown in Table 2.8. The I_Q has been calculated for 10 springs (S1-S7 and S11-S13). The remaining springs have been not included in the calculation due to the absence of isotope and/or discharge data.

	Altitude range [m a.s.l.]	Area [km ²]	Recharge rate [m ³ /s]	lc (from equation7)	lc (from equation 8)	%RA	(lc*RA)/100 (from equation7)	(lc*RA)/100 (from equation8)	lr (From equation 7)	lr (From equation 8)
2001	<600 m	55	0.3	-8.9	-7.3	2.1	-0.2	-0.2	-10.1	-9.6
	600 m – 1000 m	340	3.7	-9.4	-8.3	21.4	-2.0	-1.8		
	1000 m – 1400 m	310	4.8	-10.0	-9.2	28.1	-2.8	-2.6		
	1400 – 1800 m	227	4.4	-10.5	-10.2	28.2	-3.0	-2.9		
	>1800	102	3.1	-11.0	-11.2	19.7	-2.2	-2.2		
2006	<600 m	55	0.1	-8.9	-7.3	0.6	-0.1	0.0	-10.3	-9.9
	600 m – 1000 m	340	1.2	-9.4	-8.3	13.6	-1.3	-1.1		
	1000 m – 1400 m	310	2.5	-10.0	-9.2	26.6	-2.6	-2.5		
	1400 – 1800 m	227	3.4	-10.5	-10.2	32.4	-3.4	-3.3		
	>1800	102	2.7	-11.0	-11.2	26.6	-2.9	-3.0		
2007	<600 m	55	0.1	-8.9	-7.3	0.7	-0.1	-0.1	-10.3	-9.8
	600 m – 1000 m	340	1.8	-9.4	-8.3	14.6	-1.4	-1.2		
	1000 m – 1400 m	310	3.8	-10.0	-9.2	26.8	-2.7	-2.5		
	1400 – 1800 m	227	4.8	-10.5	-10.2	31.9	-3.3	-3.3		
	>1800	102	3.7	-11.0	-11.2	25.7	-2.8	-2.9		
2010	<600 m	55	0.7	-8.9	-7.3	2.7	-0.2	-0.2	-10.1	-9.5
	600 m – 1000 m	340	6.1	-9.4	-8.3	23.5	-2.2	-1.9		
	1000 m – 1400 m	310	7.5	-10.0	-9.2	28.8	-2.9	-2.7		
	1400 – 1800 m	227	7.2	-10.5	-10.2	27.3	-2.9	-2.8		
	>1800	102	4.6	-11.0	-11.2	17.3	-1.9	-1.9		
2020	<600 m	55	0.1	-8.9	-7.3	0.9	-0.1	-0.1	-10.3	-9.9
	600 m – 1000 m	340	1.5	-9.4	-8.3	13	-1.2	-1.1		
	1000 m – 1400 m	310	2.7	-10.0	-9.2	26	-2.6	-2.4		
	1400 – 1800 m	227	3.6	-10.5	-10.2	33	-3.5	-3.4		
	>1800	102	2.9	-11.0	-11.2	27	-3.0	-3.0		
2021	<600 m	55	0.8	-8.9	-7.3	3.4	-0.3	-0.2	-10.1	-9.5
	600 m – 1000 m	340	6.0	-9.4	-8.3	25.7	-2.4	-2.1		
	1000 m – 1400 m	310	7.6	-10.0	-9.2	29.7	-3.0	-2.7		
	1400 – 1800 m	227	7.1	-10.5	-10.2	26	-2.7	-2.6		
	>1800	102	4.5	-11.0	-11.2	15.4	-1.7	-1.7		
2001-2020	<600 m	55	1.2	-8.9	-7.3	1.7	-0.2	-0.1	-10.2	-9.7
	600 m – 1000 m	340	3.5	-9.4	-8.3	18.9	-1.8	-1.6		
	1000 m – 1400 m	310	5.3	-10.0	-9.2	28.2	-2.8	-2.6		
	1400 – 1800 m	227	5.4	-10.5	-10.2	29	-3.0	-3.0		
	>1800	102	4.3	-11.0	-11.2	22	-2.4	-2.5		

Table 2.7: lr ($\delta^{18}O$ weighted isotope from recharge), obtained for the 2001, 2006, 2007, 2010, 2020 and 2021 years

Year	ID	Q _s [m ³ /s]	l _a	Q _s •l _a	l _Q
2001	S1	0.4	-9.1	-3.7	-9.7
	S2	0.2	-10.1	-1.8	
	S3	1.0	-9.9	-10.3	
	S4	0.7	-9.7	-6.9	
	S5	0.6	-9.7	-5.6	
	S6	0.3	-9.7	-2.4	
	S7	4.0	-9.7	-38.9	
	S11	1.2	-10.2	-12.2	
	S12	0.3	-10.4	-2.8	
	S13	1.0	-9.1	-9.0	
2006	S1	0.4	-10.3	-4.2	-10.3
	S2	0.2	-10.7	-2.1	
	S3	1.0	-10.8	-10.6	
	S4	0.5	-10.9	-5.2	
	S5	0.4	-10.6	-4.6	
	S6	0.3	-10.9	-2.9	
	S7	4.6	-10.1	-46.7	
	S11	1.3	-10.5	-13.7	
	S12	0.3	-10.6	-3.1	
	S13	1.1	-9.4	-10.4	
2007	S1	0.2	-10.6	-1.7	-10.4
	S2	0.2	-10.9	-2.0	
	S3	0.8	-11.1	-9.3	
	S4	0.4	-10.7	-4.0	
	S5	0.6	-10.8	-6.5	
	S6	0.2	-10.7	-2.5	
	S7	5.2	-10.3	-53.6	
	S11	1.2	-10.8	-13.0	
	S12	0.3	-10.8	-3.1	
	S13	1.3	-9.5	-12.4	
2010	S1	0.4	-10.9	-4.5	-10.4
	S2	0.3	-10.4	-2.7	
	S3	1.4	-11.1	-15.2	
	S4	1.2	N.M.	N.M.	
	S5	0.7	-10.6	-8.0	
	S6	0.3	-10.6	-3.1	
	S7	6.2	-10.2	-63.8	
	S11	1.3	-10.7	-14.0	
	S12	0.2	-10.5	-2.1	
	S13	0.5	-9.6	-4.3	

Year	ID	Q _s [m ³ /s]	l _a	Q _s •l _a	l _Q
2020	S1	0.04	-10.8	-0.4	-10.5
	S2	0.1	-10.6	-1.5	
	S3	0.9	-11.3	-9.9	
	S4	0.7	N.M.	N.M.	
	S5	0.5	-10.7	-5.5	
	S6	0.3	-10.8	-3.1	
	S7	5.0	-10.4	-51.8	
	S11	0.9	-11.0	-9.4	
	S12	0.2	-10.6	-1.8	
	S13	0.5	-9.1	-4.8	
2021	S1	0.1	-10.3	-0.6	-10.3
	S2	0.2	-10.4	-2.0	
	S3	0.2	-10.7	-2.5	
	S4	0.4	-10.3	-4.2	
	S5	0.3	-10.4	-3.3	
	S6	0.2	-10.5	-2.3	
	S7	4.9	-10.3	-50.4	
	S11	0.9	-10.7	-9.6	
	S12	0.1	-10.7	-1.5	
	S13	0.7	-9.6	-6.4	

Table 2.8: l_Q ($\delta^{18}O$ weighted isotope from discharge), obtained for the 2001, 2006, 2007, 2010, 2020 and 2021 years. Spring ID refer to Figure 2.2.

In Table 2.9 the isotopic results of l_Q and l_r (calculated by equations 1 and 2) are summarized.

Year	I_Q	I_r (from Barbieri et al., 2003)	I_r (from Barbieri et al., 2005)
2001	-9.7	-10.1	-9.6
2006	-10.3	-10.3	-9.9
2007	-10.4	-10.3	-9.8
2010	-10.4	-10.1	-9.5
2020	-10.5	-10.3	-9.9
2021	-10.3	-10.1	-9.5
2000-2021	-10.3	-10.2	-9.7

Table 2.9: Results of I_Q and I_r for each year and for the long-term period, summarizing the results of Table 7 and Table 8 calculations.

The Box and whisker plot in Figure 2.15 resumes the statistical distribution of real $\delta^{18}\text{O}$ values of all sampled springs for considered years. The calculated I_Q (green dots in Figure 2.15) is sufficiently in agreement with the average of real $\delta^{18}\text{O}$ data (blue numbers representing the average of the Box whiskers in Figure 2.15). This correspondence confirms that I_Q is a reliable variable with respect to measured spring discharge.

To validate the isotope recharge values obtained by meteoric data on the whole aquifer (by Thornthwaite method), the two I_r calculated through Eq. 7 and 8 have been compared with I_Q (discharge-related parameter) and real isotope values. Indeed, the I_r calculated from Eq. 7 by Barbieri et al., 2003 (red dots in Figure 2.15) are characterized by 2001 values significantly lower than I_Q . Very similar values of the two variables have been obtained for 2006, while since 2007 slightly higher I_r values are noted with respect the I_Q discharge ones. This general good agreement can be considered as an index of positive validation of the recharge methods by isotope analysis. Their difference during the observed period is an expression of the limited uncertainty of the methods and consequently of the assumed water budget of the Gran Sasso aquifer.

The alternative I_r calculated from Eq. 8 by Barbieri et al., 2005 (yellow dots in Figure 2.15) are higher than both I_Q and 75th percentile of real isotope data for each year. Note that there is an increase with time of the drift of I_r calculated by Eq. 8 (yellow dots in Figure 2.15) with respect to the median values (blue numbers in Figure 2.15).

This drift would be attributed to different causes (discrepancy in real data, uncertainties due to the applied methodology, etc.), but it can be also due to a real change in isotope content, e.g. to the migration of the stable isotope ratio towards more negative values. This last explanation is also supported by the elaboration reported in Figure 2.12, where a change of correlation of real isotope data with respect to different local meteoric water lines can be observed since 2001 to 2021. This pattern should agree with the hypothesis that the average recharge isotope altitude has been increased over the past twenty years, testifying some significant modifications of the recharge mechanism, possibly related to climate change effects on the study area.

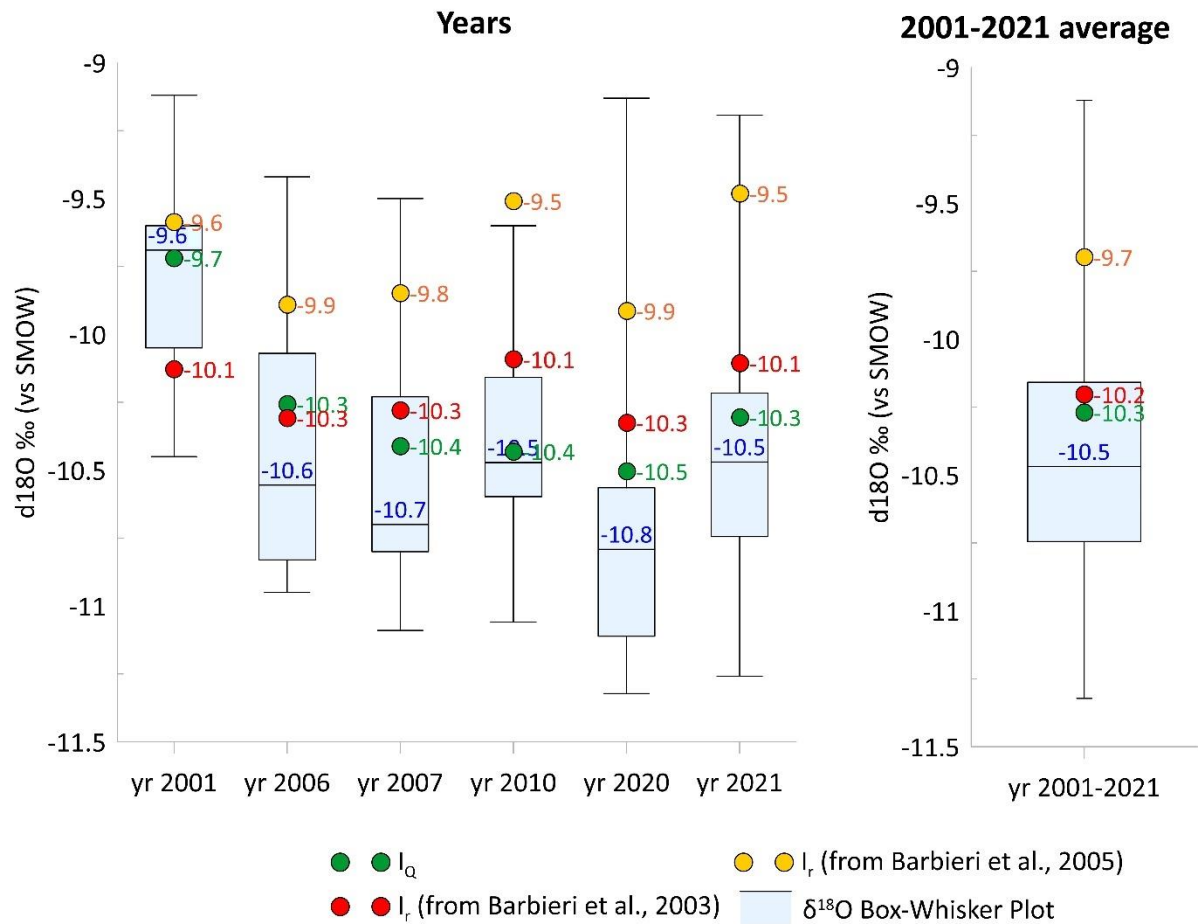


Figure 2.15: Box plot and whisker plot of $\delta^{18}O$ real values (blue numbers) compared with I_q (green dots) and I_r (yellow and red dots, respectively applying Barbieri et al., 2005 equation and Barbieri et al. 2003 equation).

2.5 Conclusions

The results of the water budget analysis computed with three different approaches (Turc, Thornthwaite, and Aplis), are very similar to each other. To verify the reliability of the obtained recharge rates, the total spring discharge and recharge calculated by three methods have been compared. Considering the correlation coefficient obtained by Thornthwaite method (Figure 14) and the related parameters (e.g., field capacity and recharge on monthly basis, Thornthwaite, 1957) this method has been considered the most reliable. For this reason, the recharge obtained by Thornthwaite method has been selected for the validation process.

A water budget validation can be carried out by different methodologies, but due to the hydrogeological complexity and extension of the Gran Sasso aquifer, the hydrogeochemical approach has been identified as the most suitable method to consider both uncertainties and validation of water budget. The adopted hydrogeochemical procedure is based on the comparison among: i) $\delta^{18}O$ computed isotope values calculated for recharge data by Thornthwaite method (I_r , Eq. 1), applying local empirical CIRE (Computed Isotope Recharge Elevation) equations, ii) computed averaged $\delta^{18}O$ from discharge of each spring (I_q , Eq. 2), and iii) real isotopic values (I_m) collected during this study and during previous samplings. This isotopic procedure (Figure 15) leads to a good correspondence between I_q and I_m , confirming the reliability of the discharge assessment of the study. The comparison between I_r values and real isotopic values I_m , reveals some differences between the two adopted CIRE equations. However, trends and variations of I_r seem to be coherent with I_m data, validating the

recharge assessment and consequently limiting the uncertainties in water budget for the Gran Sasso aquifer. Furthermore, the adopted methodology sheds light on a possible temporal isotopic dynamicity of the groundwater system. In detail, the observed drift of I_r values would be interpreted as an artifact derived from the obsolescence of used CIRE equations. Indeed, in the last twenty years real $\delta^{18}\text{O}$ values become more negative, perhaps due to possible increase of average recharge isotope altitude.

2.6 References

- Amoruso, A., Crescentini, L., Petitta, M., & Tallini, M. (2012). Parsimonious recharge/discharge modeling in carbonate fractured aquifers: The groundwater flow in the Gran Sasso aquifer (Central Italy). *J. Hydrol.* 476, 136–146
- Andreo B., Vias J., Duran J., Jimenez P., Lopez-Geta J.A., Carrasco F. (2008). Methodology for groundwater recharge assessment in carbonate aquifers: application to pilot sites in southern Spain. *Hydrogeol J.* 16, 911-925.
- Amoruso, A., Crescentini, L., Petitta, M., & Tallini, M., (2012). Parsimonious recharge/discharge modeling in carbonate fractured aquifers: The groundwater flow in the Gran Sasso aquifer (Central Italy). *J. Hydrol.* 476, 136–146.
- Barbieri M., Petitta M., D’Amelio L., Desiderio G., Rusi S., Marchetti A., Nanni T., Tallini M. (2003). Gli isotopi ambientali (^{18}O , ^2H , e $^{87}\text{Sr}/^{86}\text{Sr}$) nelle acque sorgive dell’appennino Abruzzese: considerazioni sui circuiti sotterranei negli acquiferi carbonatici. Atti I° Convegno Nazionale, AIGA, 69-81.
- Barbieri M, Boschetti T, Petitta M, Tallini M (2005) Stable isotope (^2H , ^{18}O and $^{87}\text{Sr}/^{86}\text{Sr}$) and hydrochemistry monitoring for groundwater hydrodynamics analysis in a karst aquifer (Gran Sasso, Central Italy), *Appl. Geochem.* 20: 2063-2081.
- Celico P, Gonfiantini R, Koizumi M, Mangano F (1984) Environmental isotope studies of limestone aquifers in central Italy. Proceedings of International Symposium on Isotope Hydrology in Water Resource Development. I.A.E.A., Vienna.
- Fazzini M., Bisci C. (1999). Clima e neve sul massiccio del Gran Sasso. *Neve e Valanghe*, Vol. 36
- Longinelli, A., and Selmo, E. (2003). Isotopic composition of precipitation in Italy: a first overall map. *Journal of Hydrology*, 270(1-2), 75-88.
- Mazzilli, N., Guinot, V., Jourde, H., Lecoq, N., Labat, D., Arfib, B., Baudement, C., Danquigny, C., Dal Soglio, L., Bertin, D. (2019). KarstMod: a modelling platform for rainfall-discharge analysis and modelling dedicated to karst systems. *Environmental Modelling & Software*, 122, 103927.
- Petitta, M., Tallini, M. (2002). Groundwater hydrodynamic of the Gran Sasso Massif (Abruzzo): New hydrological, hydrogeological and hydrochemical surveys (19994-2001). *Boll Soc Geol It* 121, 343-363.
- Scozzafava, M., & Tallini, M. (2001). Net infiltration in the Gran Sasso Massif of central Italy using the Thornthwaite water budget and curve-number method. *Hydrogeol J.*, 9, 461–475.
- Sivelle, V., Jourde, H., Bittner, D., Mazzilli, N., & Trambly, Y. (2021). Assessment of the relative impacts of climate changes and anthropogenic forcing on spring discharge of a Mediterranean karst system. *Journal of Hydrology*, 598, 126396.
- Thornthwaite, C.W. & Mather, J.R. (1957). Instructions and tables for computing potential evapotranspiration and the water balance. *Publ. Climatol.*, 10.
- Turc, L. (1954). Le bilan d’eau des sols : Relations entre les precipitations, l’évaporation et l’écoulement. *Annales Agronomiques*, 5, 491-595 ; 6, 5-131.

3 The Djebel Zaghouan aquifer (Case Study Tunisia)

3.1 Study Area

The Djebel Zaghouan is the most important Jurassic of the Zaghouan massif and it is located at about fifty kilometers from Tunis (Tunisia). This massif is constituted by monoclinals of limestone overlapping one on the other. It is also made of marls of the Cretaceous and Eocene (Castany, 1951). The Djebel Zaghouan is characterized by the presence of southern and transverse faults that have created individualized blocks. These faults allow the infiltration. The Zaghouan karst aquifer is about 19.6 km² area (**Errore. L'origine riferimento non è stata trovata.**). It has an eastern part favorable to the storage of seepage water, contrary to its western part, its western part where marl deposits strongly decrease the storage coefficient (Djebbi et al., 2001).

The geology of Djebel Zaghouan has made it an important water reserve used since antiquity for the water supply of Carthage, then Tunis. The Roman aqueduct (120 A.D.), still very well preserved, which connects the water temple to the city of Carthage, can be seen along the road linking Tunis to Zaghouan. Currently, the aquifer is exploited by mainly 9 boreholes and galleries intended for the drinking water supply of the city of Zaghouan and the surrounding rural agglomerations. Three of these wells used as commercialized mineral water.

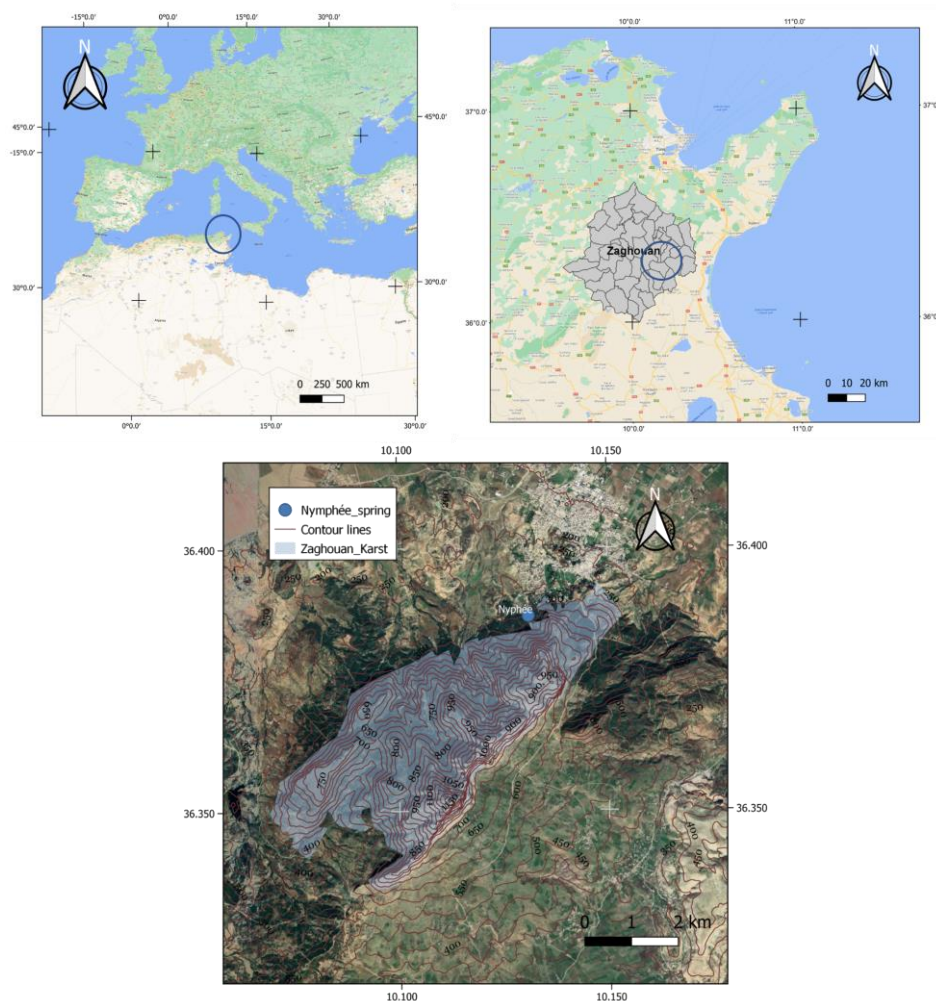


Figure 3.1. Location of the Djebel Zaghouan karst aquifer

3.2 Water Budget Summary

The water budget was principally based on the modeling study performed by Djebbi et al. (2001) and Sagna (2000). This study proposed to assess the water balance and to quantify the storage capacity of the aquifer associated with the Jurassic limestones of Djebel Zaghuan. The available flow data corresponding to the natural flow period was recorded from 1915 to 1927. Table 3.2 and

Table 3.3 presents the Zaghuan springs production before the digging of the galleries and Zaghuan springs production with exploitation by the galleries respectively. The natural flow period was marked by heavy rainfall of the 1920-1921 and a low rainfall during the 1926-1927 hydrological years, which resulted in high spring flow (6.5 Mm^3) and a very low flow of 1.9 Mm^3 respectively. These observations are in conformity with the natural flow of the resurgences during this period.

Table 3.2 : Zaghuan springs production before exploitation by the galleries

Production (Mm^3)	
Year	Total
1915-1916	3.5
1916-1917	3.3
1917-1918	3.3
1918-1919	3.7
1919-1920	3
1920-1921	6.5
1921-1922	4.8
1922-1923	3.9
1923-1924	3.8
1924-1925	2.9
1925-1926	3
1926-1927	1.9
Average	3.6
Standard deviation	1.1

Table 3.3 : Zaghouan springs production with exploitation by the galleries

Production (Mm ³)	
Year	Total
1970-1971	4
1971-1972	3.9
1972-1973	5
1973-1974	5.9
1974-1975	4.2
1975-1976	3.7
1976-1977	3.2
1977-1978	2.4
1978-1979	1.9
1979-1980	1.3
1980-1981	1.5
1981-1982	2.4
1982-1983	6.2
1983-1984	2.9
1984-1985	3.3
1985-1986	2.9
1986-1987	2.1
1987-1988	1.9
1988-1989	1.6
1989-1990	1.9
1990-1991	3.3
1991-1992	4.2
1992-1993	3.4
1993-1994	2.9
1994-1995	1.9
Average	3.1
Standard deviation	1.3

Sagna (2000) considered the most continuous and overlapping series of both dry and wet years. The average interannual rainfall calculated over a time series of 47 years was 501 mm with a standard deviation of 170 mm. Observations were recorded at the TPSM rainfall station. Temperature was taken from bibliography and monthly mean evapotranspiration was calculated using Thornthwaite formula.

Djebbi et al. (2001) and Sagna (2000) also developed a conceptual deterministic model to transform the rainfall received by the calcareous solid mass into the sum of the discharge flows (springs and galleries). The model was validated using meteorological and hydrodynamic collected data. Calculation time step is daily. Model was run for a calibration period corresponding to the natural functioning of the system from 1915 to 1927 and a validation period from 1970 to 1995 including the aquifer exploitation via galleries and wells. The performance of the model was acceptable with a Nash criterion ranging between 0.54 % and 0.77 %.

Table 3.4 and Table 3.5 provides Djebel Zaghouan water budgets summary (rainfall, infiltration rate, runoff and evapotranspiration) for the calibration and the validation period respectively. It provides (all of which represent the components of a natural water budget (1915-1927)) (Sagna, 2000), after the classical methodology of calibration and final validation in the model.

Table 3.4: Water budget for the calibration period (1915-1927)

Year	Rainfall (mm)	Flow (Mm ³ /an)	RET (Mm ³)	Runoff (Mm ³)	Water budget (%)	Infiltration coefficient (%)
1915-1916	480	3.4	4.5	0.37	110	38
1915-1917	461	3	6.1	0.21	93	35
1915-1918	442	3	4.8	0.29	103	36
1915-1919	550	4	4.8	0.45	113	38
1915-1920	347	3	4.7	0.15	83	47
1915-1921	867	5.2	7.1	0.75	126	31
1915-1922	393	5	3.4	0.32	84	68
1915-1923	400	4	4.1	0.28	91	53
1915-1924	525	4.4	4.8	0.41	103	45
1915-1925	380	3.4	4.8	0.2	86	48
1915-1926	520	2.9	7	0.21	95	30
Average	488	3.8	5.1	0.33	99	43

Table 3.5: Water budget validation of model (1970-1995)

Year	Rainfall (mm)	Flow (Mm ³ /an)	RET (Mm ³)	Runoff (Mm ³)	Water budget (%)	Infiltration coefficient (%)
1970-1971	448	4.3	3.2	0.42	93	50
1971-1972	642	5.3	5.7	0.51	94	43
1972-1973	686	6	5.2	0.6	92	46
1973-1974	547	5.9	4.9	0.4	108	57
1974-1975	472	4.7	4.6	0.3	109	53
1975-1976	506	4	6.2	0.3	110	42
1976-1977	341	3	4.1	0.2	114	48
1977-1978	373	2.5	5.1	0.16	110	35
1978-1979	352	2.3	4	0.2	98	34
1979-1980	425	1.9	6.7	0.1	108	23
1980-1981	339	1.9	4.3	0.17	99	30
1981-1982	409	2.3	4.6	0.25	92	30
1982-1983	641	5.5	3.4	0.7	79	46
1983-1984	252	2.7	4.6	0.02	154	57
1984-1985	551	3.2	5.8	0.37	90	31
1985-1986	334	2.5	4.5	0.15	113	40
1986-1987	498	3	5.7	0.3	96	33
1987-1988	232	1.6	4.4	0	137	37
1988-1989	273	1	4.1	0.05	101	21
1989-1990	609	2.5	7	0.39	86	21
1990-1991	567	4.4	4.3	0.52	85	40
1991-1992	687	4.8	7.6	0.44	98	37
1992-1993	463	3.8	5.6	0.26	110	44
1993-1994	292	2.7	4.1	0.1	126	49
1994-1995	192	1.4	3.6	0	138	38
Average	445	3.3	4.9	0.28	106	39

Recharge rates issued from the conceptual model for the natural flow period ranged from 30% to 68% (average 42 %). For the period corresponding to the functioning of the system via galleries by regulating valves, the infiltration rates varied between 21% and 57 % (average 39.4 %).

Using the APLIS method, the majority of the study area has estimated infiltration rates in the “moderate” category (40–50 %) (Figure 3.1). The overall infiltration rate for the study area is 45%. Despite, the uncertainties of measurements of discharges and flow and climatic data processing, APLIS method gave recharge rates of the same range as the values calculated by the model.

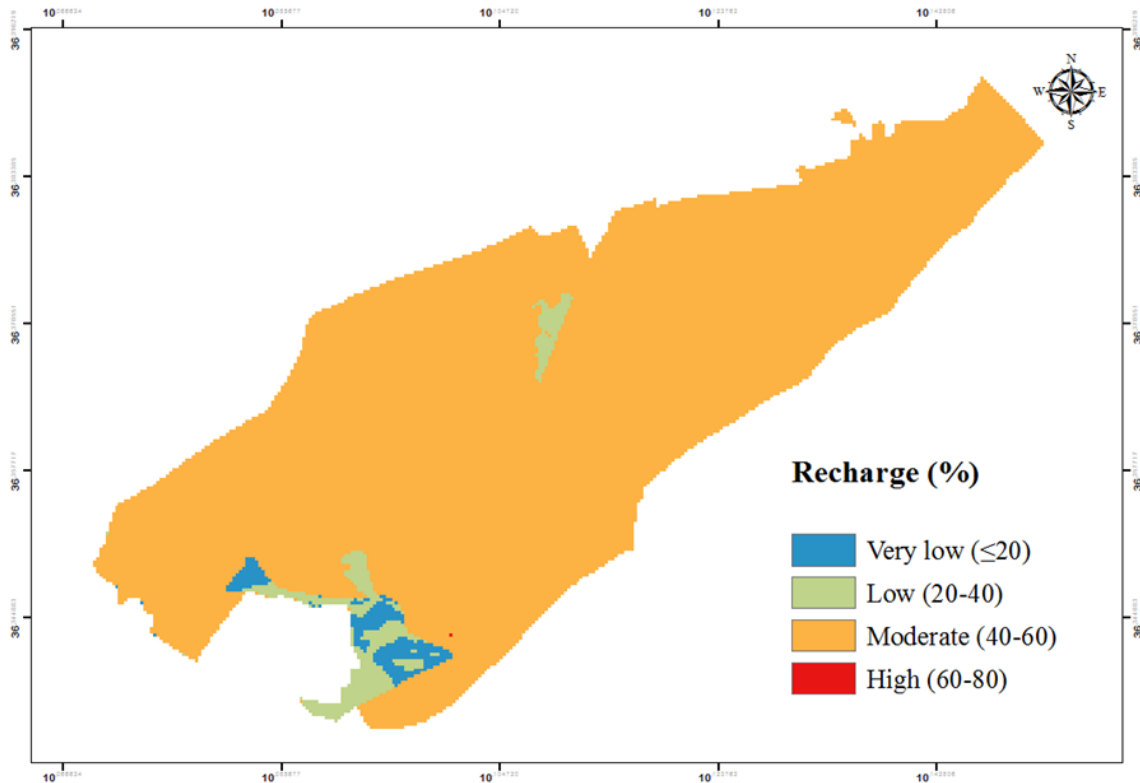


Figure 3.1 : Groundwater recharge distribution by the APLIS method

3.3. Weakness and uncertainties of the adopted methods

Errors and uncertainties are principally due to methods and time step measurement as well as data processing. Indeed, discharge series were available in graphical form (Figure 3.2) from 1915 to 1927 at irregular time scales. Discharges were then obtained by linear interpolation on a daily scale. Thus, several sources of uncertainties are issued from the rough data and its interpolation. In fact, measurements were taken on a weekly, twice-weekly, or once-monthly basis rather than daily (Figure 3). Besides, we can cite uncertainties related to the measurement techniques used at the beginning of the 20th century and based on weirs and their calibration curves.

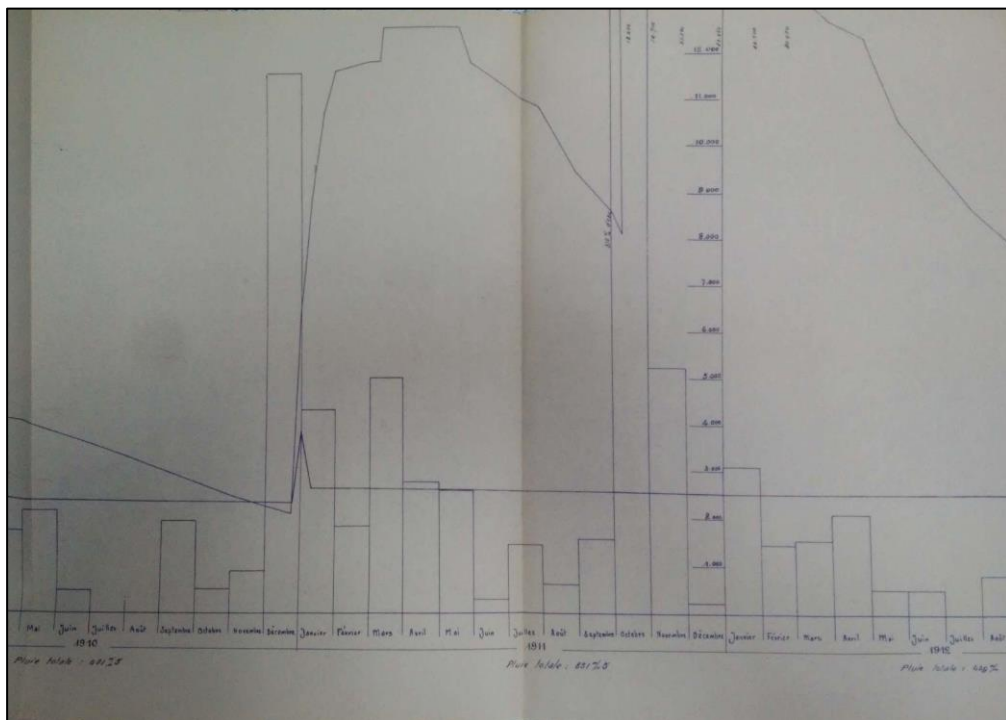
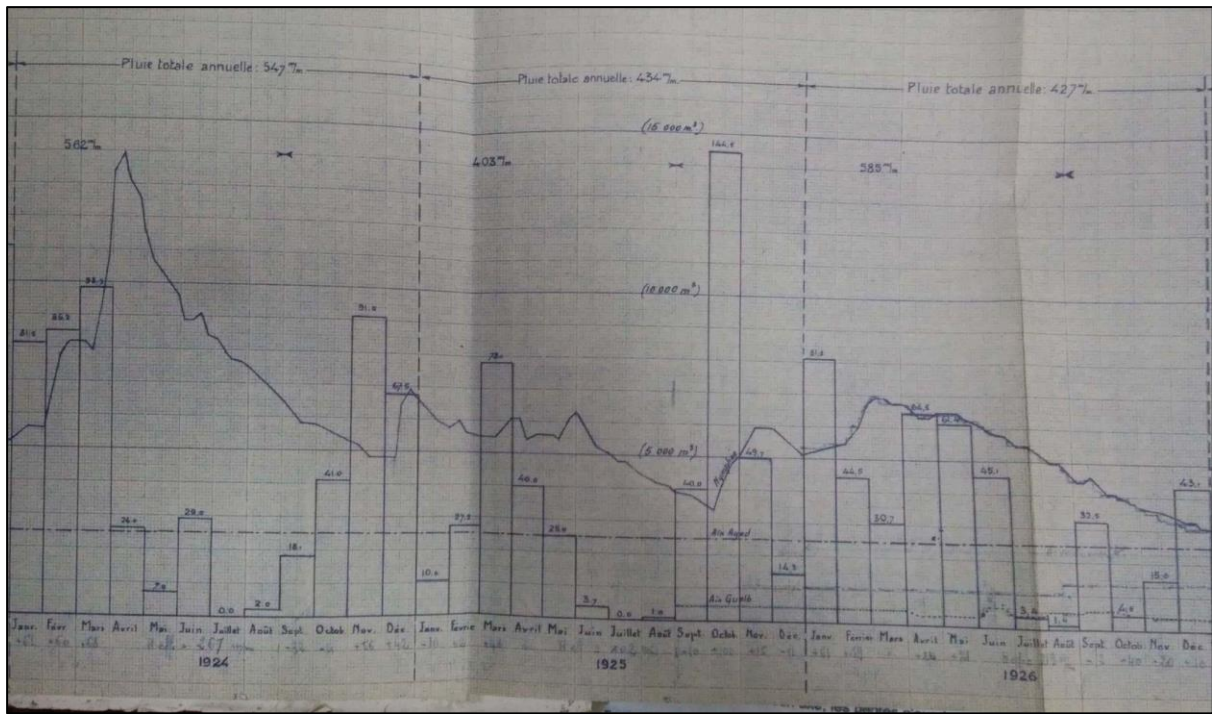


Figure 3.2: Examples of non-digitized discharge from 1915 to 1930

Besides, and since the installation of the valves to control the flows supplied by the galleries, the system is no longer natural. The flows observed from 1958 to 1962 and from 1971 to 1995 are very random and indicate that they are highly dependent on the openings of the gates. These openings depend on several contingencies, in particular the daily demands made by SONEDE to meet the water needs of its users.

The rainfall data comes from the TPSM station, which is situated at 184 meters altitude. They span the years March 1908 to August 1998, but there are significant gaps in the data. Records from the nearby DGRE station have helped fill in some of the gaps.

Due to the lack of daily potential evapotranspiration data, it was calculated on a monthly scale using Thornwaith's method based on monthly mean temperatures and the massif's latitude. The average monthly temperatures were taken at the Kébir dam, which is 37 kilometers from Zaghouan.

3.4. Conclusion

In this report we summarized the water budget results, compared results of recharge rates issued from a conceptual model and APPLIS method. Potential uncertainties related to water budget estimation were discussed. To improve the water budget estimation, the graphical data were completed from SONEDE archives and digitized. Monthly mean temperatures for a number of years corresponding to the natural functioning of the system were collected from the national archives. The ongoing geological, geophysical and isotopic investigations should also

- Allow better understanding of the overall functioning of the karstic system
- Improve the delineation of the adopted aquifer boundaries.
- Improve the estimation of the water budget

3.5 References

- Castany, G., 1951. Djebel Zaghouan, carte géologique. Dans: S. g. d. Tunisie-Tunis, éd. Étude géologique de L'Atlas Tunisien Oriental. Tunis: Tunisie. Service géologique. Éditeur scientifique, p. 1.
- Djebbi M. , Sagna J. and Besbes M. (2001). Sources karstiques de Zaghouan : Recherche d'un opérateur Pluie - Débit. Sciences Et Techniques De L'Environnement Mémoire Hors-Serie,
- Dziri R., Chkir N., Emblanch C., Zouari K. and Gallali A. (2016). Geochemical and hydrodynamic characteristics of the karstic system of Jbal Zaghouan (Northeastern-Tunisia). I-DUST 2016: inter-Disciplinary Underground Science & Technology Avignon
- Nazoumou Y., (2002). Study of the deep aquifers of the South-Eastern Governorate of Zaghouan (Tunisia). Report, Water Resources Directorate /SCET-Tunisia, Tunis, TUNISIA, 100 p.
- Nazoumou Y., (2002). Water resources database of the South Delegations- East of the Governorate of Zaghouan (Tunisia). Report, Directorate of Resources in Water / SCET-Tunisia, Tunis, TUNISIA, 100 p.
- Sagna J., (2000), Study and modeling of Zaghouan karst sources, Master thesis. ENIT. 84 p.

4 The Qachqouch aquifer (Case Study Lebanon)

4.1 Study Area: The Qachqouch spring

Qachqouch Spring (Figure 4.1), is located within the Nahr el Kalb Catchment and originates from the Jurassic karst aquifer at about 64 meters above sea level. During low flow periods, the spring is used to complement the water deficit in the capital city Beirut and surrounding areas. Its total yearly discharge reaches 35-55 millions of m^3 based on high-resolution monitoring of the spring (2014-2019; Dubois et al., 2020). Flow maxima reach a value of $10 m^3/s$ for a short period following flood events; discharge is about $2 m^3/s$ during high flow periods and $0.2 m^3/s$ during recession periods.

About 67% of the area in Lebanon consists of karstified ($6,900 km^2$) rock sequences (Dubois, 2017). The catchment area drained by the Qachqouch spring is delimited to the North by Nahr El Kalb River and extends for more than $55 km^2$ of mountainous nature at a maximum elevation of 1650 m.a.s.l. (Dubois, 2017). Tracer experiments show a relationship between the Nahr El Kalb River and the Qachqouch Spring through a sinking stream (Doummar and Aoun, 2018b).

The spring originates from a carbonate aquifer composed of the Jurassic formation sequence of massive fissured limestone of more than 100 m in thickness. Dolostones characterized by a higher porosity (10-12%) are found in the lower part of the formation because of the diagenetic dolomitization and along leaky faults and dykes because of hydrothermal dolomitization (Nader et al., 2004). The area is characterized by a duality of infiltration portrayed by the point source infiltration in preferential pathways (dolines, permeable faults) and diffuse recharge in bare fissured rocks.

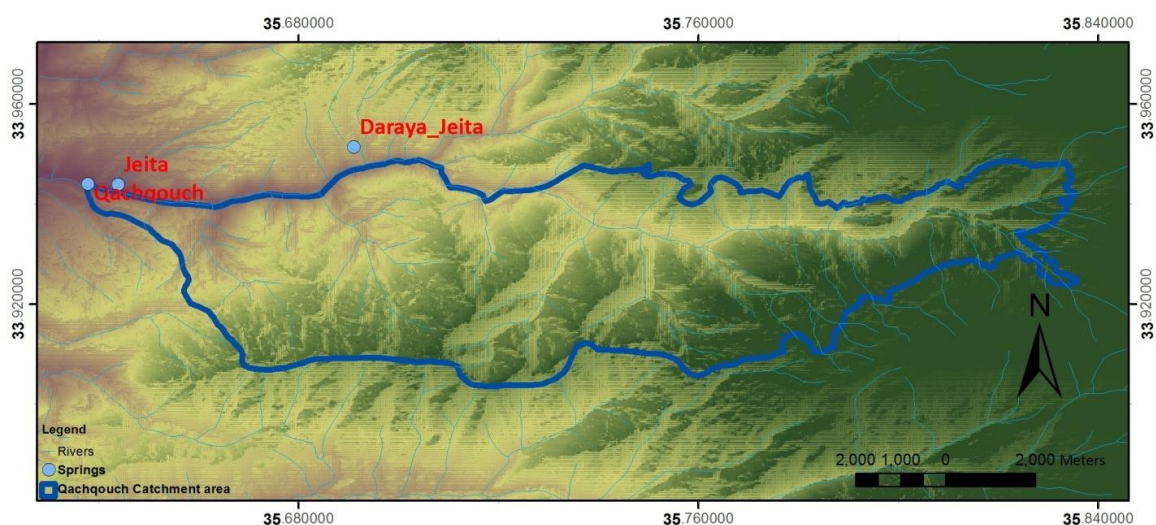


Figure 4.1. The catchment area of the investigated Spring (Qachqouch). Nahr el Kalb River acting as a boundary condition in the northern part of the catchment. Catchment tentatively delineated encompassing autochthonous recharge occurring in Jurassic and lower cretaceous rock exposures.

4.2 Water Budget Result Summary

Three main methods were used to estimate recharge on the Qachqouch Catchment: 1) The Water Balance Method, 2) the APLIS Method, 3) the Numerical Modelling Approach. Additionally, the analysis of stable isotopes allowed to define the recharge elevation and infiltration that was not considered in the original delineation of the spring catchment.

With the APLIS method, the total recharge over the catchment area amounted to about 22-28 Mm^3 for a dry and wet year respectively (Table 4.1). The amount of specific recharge per area was

successfully estimated using APLIS for the catchment area of Qachqouch and revealed that substantial recharge (60% and above of precipitation) occurs on a large area over the Spring catchment, indicative of its karstic nature and predominance of point source infiltration. The water balance method that accounts for the components of the hydraulic cycle; namely, real evapotranspiration, surface runoff, which is considered negligible in the study area, due to a high karstification, and the spring discharge that ranged between 35 and 50 Mm³ during average years, with extremes in very wet years (Table 4.2). The high discharge estimated during very wet years is due to errors in flow measurements (and calibration of the water stage during flood). Thus, it is considered that the calculated discharge during years where P exceeds 1000 mm has some uncertainties that can only be resolved with numerical modelling or from a statistical calculation of classified flowrates performed on the 2016-2018 time series (Dubois et al., 2020).

Table 4.1 Recharge classes, areas, and total average recharge values in m³ per class area and as a percentage of the total area (A_t) as computed with APLIS

Class (mm)	Wet year			Dry year			Intermediate year		
	Area (km ²)	Volume (Mm ³)	% of A _t	Area (km ²)	Volume (Mm ³)	% of A _t	Area (km ²)	Volume (Mm ³)	% of A _t
0-200	17.64	1.8	34%	17.64	1.8	34%	17.64	1.8	34%
200-400	0.97	0.3	2%	1.41	0.4	3%	0.01	0.0	0%
400-600	4.40	2.2	8%	15.17	7.6	29%	6.12	3.1	12%
600-800	14.20	9.9	27%	17.55	12.3	34%	22.44	15.7	43%
800-1000	14.24	12.8	27%	0.05	0	0%	5.62	5.1	11%
1000-1200	0.38	0.4	1%	0.00	0	0%	0.00	0.0	0%
Total (Mm³)		27.5	±5 Mm³		22.1	±5 Mm³		25.6	±5 Mm³

*A_t=51 km²

The modelling approach using a lumped model with three reservoirs yielded similar results to the water balance methods for the years 2016-2018 (Dubois et al., 2020). In the baseline scenario (2016-17), the modelled precipitation, and evapotranspiration were respectively 966 mm, and 167 mm (17.2%) over a total catchment area of 56 km². The change of precipitation by -10% yields an error in evapotranspiration of 6.2% with respect to the baseline scenario and an error of discharge of 11% (Table 4.3).

Table 4.2 Preliminary water balance assessment for the Qachqouch catchment (the spring being the only outlet)

Total Precipitation (mm) Value at 950 m asl	Recharge Q (Qachqouch)	Real Evapotranspiration (%)
921 mm (2015-16)	35 Mm ³ (2015-16)-652 mm (70%)	10-30% of total budget
1034 mm (2016-17)	47 Mm ³ (2016-17)- 839 mm (81%)	
1089 mm (2017-18)	50 Mm ³ (2017-18)- 892 mm (81%)	
Very Wet year	105 Mm ³ (? Too high) High uncertainties in high flow measurements	
1838 mm (2018-19)	81.3 Mm ³ (? Too high)- High uncertainties in high flow measurements	
1405 mm (2019-20)		
1160 mm (2020-21)	49.8 Mm ³ 890 mm (77%)	

Table 4.3 Simulation results and comparison of model output with changes of model input in comparison with the baseline scenario (Dubois et al. 2020).

No.	Name	Scenarios Condition	Precipitation (mm yr ⁻¹)	Average annual discharge flow			Actual evapotranspiration (mm yr ⁻¹)	Duration of the summer low flow (days < 0.2 m ³ s ⁻¹)
				(mm yr ⁻¹)	(m ³ s ⁻¹)	in comparison with the baseline scenario		
-	Baseline	Invariant precipitation, temperature, and ET rates (average climatic year)	966	837	1.49	-	167	112
1	Precipitation -10%	Cumulative decrease of 10% in the precipitation rate over 10 years	873	745	1.33	-11%	163	118
2	Precipitation -30%	Cumulative decrease of 30% in the precipitation rate over 10 years	679	556	0.99	-34%	152	133
3	Temperature +1 °C	Cumulative increase in temperature of 1 °C over 10 years and the associated evolution of ET rates	966	828	1.47	-1%	176	114
4	Temperature +3 °C	Cumulative increase in temperature of 3 °C over 10 years and the associated evolution of ET rates	966	811	1.44	-3%	194	115
5	Precipitation -10% and temperature +1 °C	Combination of 1 and 3	873	736	1.31	-12%	171	119
6	Precipitation -30% and temperature +3 °C	Combination of 2 and 4	679	532	0.95	-36%	175	137
7	Increased intensity of precipitation	Sum of the baseline precipitation per 3 d (annual precipitation constant)	960	879	1.57	+5%	118	102

4.3 Weakness and uncertainties of the adopted methods

On the one hand, the amounts estimated using the APLIS method were underestimated with respect to the water balance and numerical modelling approach. The recharge may vary according to the rain intensity, overland flow from layers outside the catchment, and saturation in the subsurface. However, the amount of recharge estimated using APLIS fall well within the ranges of spring discharge. A sensitivity analysis will allow a better understanding of the effect of varying APLIS parameters on the resulting recharge map. On the other hand, the reported recharge using numerical modelling bears an

error of 11 percent for precipitation rates below 1000 mm, however for very wet years, the uncertainties in discharge measurements yield very high errors in the estimation of the total yearly discharge and consequently affect the water balance methods. Only numerical modelling allows to constraints the flow during high flow as to limit the uncertainties due to measurements (Table 4.4).

The delineation of the catchment area plays an important role in the assessment of total recharge in all the adopted methods. The catchment was outlined based on geological information and conceptual boundary conditions (River, catchments of adjacent non-connected springs etc.), however information from isotopic signatures show that the spring receives a snow component which can be better quantified with a longer time series. The values of $\delta^{18}\text{O}$ and $\delta^2\text{H}$ vary respectively between -7.67 and -6.08‰, and -36.16 and -23.61‰ with means of 6.58 ‰ and 28.48 ‰ for n=141 samples. The distribution of stable isotopes values helps assess qualitatively the extent of the catchment, indicating altitudes ranging between 1000 and beyond 1500 m, which extends beyond the Jurassic Aquifer exposure.

Table 4.4 Limitations and advantages of the used methods in the estimation of recharge on the Qachqouch catchment

Method	Advantages	Limitations and suggestions
Water Balance	Relies on the spring discharge yearly volumes and an estimation of evapotranspiration Easy estimation of recharge	Uncertainties in catchment delineation and area Daily discharge values during flood periods impact yearly discharge volumes Lumped estimation of recharge
APLIS method	Provides a spatial distribution of recharge according to precipitation Allows computing the specific recharge per unit area.	Static recharge estimation that does not account for a change in precipitation intensity and overland flow Requires high resolution detailed raster coverage of parameters influencing recharge, especially infiltration
Numerical modelling (semi-distributed lumped model)	If calibrated and validated, a model allows to estimate daily recharge to a precipitation input. It allows constraining the uncertainty in the high flow discharge rates	Catchment delineation and area Daily discharge values during flood periods impact yearly discharge volumes Required calibration and validation and a proper parameterization
Isotopes	Provides information about catchment altitude, ratio of mixing. Can be used to quantify fast infiltration percent of precipitation, and river input with a high-resolution long-time series.	Does not allow to calculate total recharge

The tracer experiments have shown that the river contributes from 3-5 % to the flow in the spring (Doummar and Aoun, 2018b). However, since the river fed by snowmelt from April to June, infiltrates into a sinking stream in the lower parts of the catchment and influences the stable isotope signature in the spring, the differentiation between allochthonous and autochthonous discharge can be done based on the detailed analysis of isotopic time series over more than a year. An infiltration of overflow may also occur in the Jurassic downstream exposures allowing for a delayed recharge and an increased storage effect (Dubois et al., 2020). Additionally, previous isotopic studies have shown that a ratio of more than 75 % should be coming from high altitudes than 800 m rather from the direct catchment at lower altitudes. This is in accordance with the presence of dolostones and point source infiltration (dolines) at these altitudes. Therefore, the area of the catchment may be higher than expected, or overland flow needs to be accounted for while computing the water balance of the Qachqouch Spring.

4.4 Conclusion

Based on the analysis of the different methods used to estimate recharge on the Qachqouch catchment, it is highly recommended to perform statistical analysis on the discharge time series (classification of flow rates) to correct for the overestimated discharge values during flood periods. The latter impact the total yearly discharge especially during very wet years. With better estimates of yearly discharge values, the combination of the water balance method and the analysis of isotopic ratio in high resolution time series allows an educated estimation of the size of the catchment area, including allochthonous and autochthonous recharge. Thus, this additional information can help refining the total recharge and recharge per unit area computed with the APLIS method, thus reducing the gap between the total yearly discharge and total recharge observed in APLIS. Finally, the delineation of the catchment area plays an important role only in semi-distributed lumped models, however calibrated and validated lumped linear reservoir models can help estimate recharge with the least uncertainties among all the other adopted methods.

4.5 References

Doummar, J. and Aoun, M. Occurrence of selected domestic and hospital emerging micropollutants on a rural surface water basin linked to a groundwater karst catchment, *Environmental Earth Sciences*, 77(9), 351, doi: 10.1007/s12665-018-7536-x, 2018b.

Dubois E., Doummar J., Pistre S., Larocque M. Calibration of a semi-distributed lumped model of a karst system using time series data analysis: the example of the Qachqouch karst spring. *Hydrol. Earth Syst. Sci.*, 24, 4275–4290, doi.org/10.5194/hess-24-4275-2020, 2020.

Dubois, E: Analysis of high-resolution spring hydrographs and climatic data: application on the Qachqouch spring (Lebanon), Master thesis, American University of Beirut, Department of Geology, Beirut, Lebanon. 2017. [online] Available from: https://www.researchgate.net/profile/Emmanuel_Dubois5/publication/320237930_Analysis_of_high_resolution_spring_hydrographs_and_climatic_data_application_on_the_Qachqouch_spring_Lebanon/links/59d69a76a6fdcc52aca7d05c/Analysis-of-high-resolution-spring-hydrographs-and-climatic-data-application-on-the-Qachqouch-spring-Lebanon.pdf, 2017

5 Eastern Ronda Mountains and Ubrique test site (case study Spain)

5.1 Study Area

The **Eastern Ronda Mountains** test site is located approximately 20 km to the east of the Ronda city (western area of Málaga province) and is composed by three Sierras (Merinos-Colorado-Carrasco, Fig. 5.1) that present a NE-SW alignment with steep slopes that range from 800 to 1200 m.a.s.l. The geological structure is constituted by box-type folds, oriented NE-SW and plunging toward NE (Martín-Algarra, 1987). The hydrogeological context is defined by Jurassic limestones which cover a large area. They constitute the main aquifer lithologies and are represented on surface as karst exposures, or in depth, as buried aquifer segments. Dolomitic rocks, which comprise the lower levels of the Jurassic aquifers, can reach higher positions in the lithological sequence, and even appear on surface. Gypsum bearing formations (Triassic clays with gypsum), whose thickness is still imprecise, constitute the lower limit of the main aquifers and can uplift through faults. Recharge is produced by the infiltration of rainwater through limestone and dolostone outcrops, while discharge is made through springs located at the borders, between the permeable carbonate rocks and the impervious layers (Fig. 5.1).

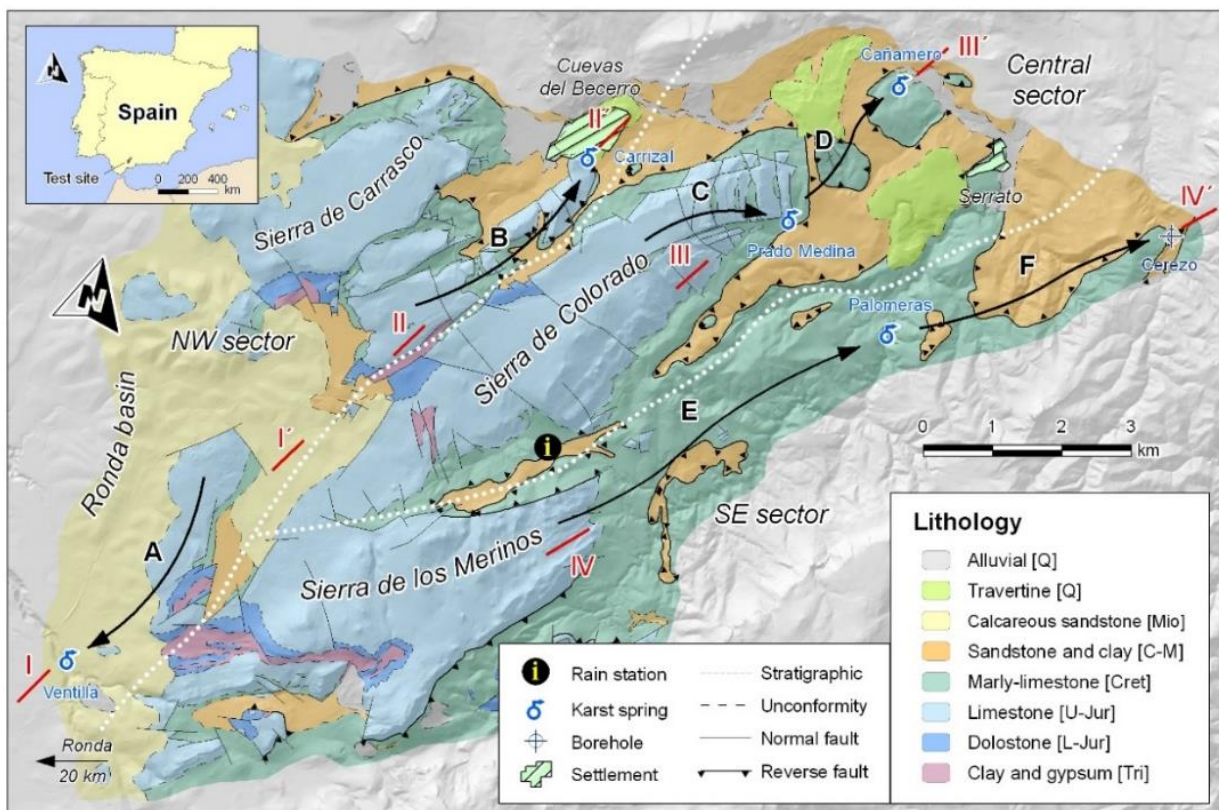


Figure 5.1. Hydrogeological setting of Merinos, Colorado y Carrasco aquifer systems (Barberá et al., 2012).

Drainage in the **Eastern Ronda Mountains** system is made in natural regime, mainly towards NE border, through the springs of Cañamero (540 m a.s.l.), Prado Medina (660 m a.s.l., an overflow type associated with the latter), Palomeras (560 m a.s.l.) and Carrizal (740 m a.s.l.). In addition, groundwater transference toward the porous aquifer of the Ronda basin (overlying the Jurassic aquifer) exists and, the shallower (visible) discharge takes place via Ventilla spring (740 m a.s.l.).

On the other hand, **Sierra de Ubrique** test site is placed within Sierra de Grazalema Natural Park, in the eastern part of the Cádiz province, 35 km of distance from the main study area and 80 km NE from Cádiz city. The lithologies that constitute the main aquifer formations in this area are also constituted by Jurassic dolostones and limestones, resulting in highly fractured and karstified systems (Martín-Rodríguez et al., 2016). Geological structure is defined by NE-SW direction folds in which anticline core dolostones and limestones are found, while cretaceous marls outcrop in syncline part. In this case, recharge takes place mainly by the infiltration of rainwater through limestone outcrops and an allogenic recharge which enters the system through Villaluenga del Rosario shaft. Drainage in the Sierra de Ubrique aquifer system is made through the springs Cornicabra (349 m a.s.l.), Algarrobal (317 m a.s.l.) and Garciago (422 m a.s.l., an overflow type associated with the two previous springs) (Marín et al., 2020) (Fig. 5.2).

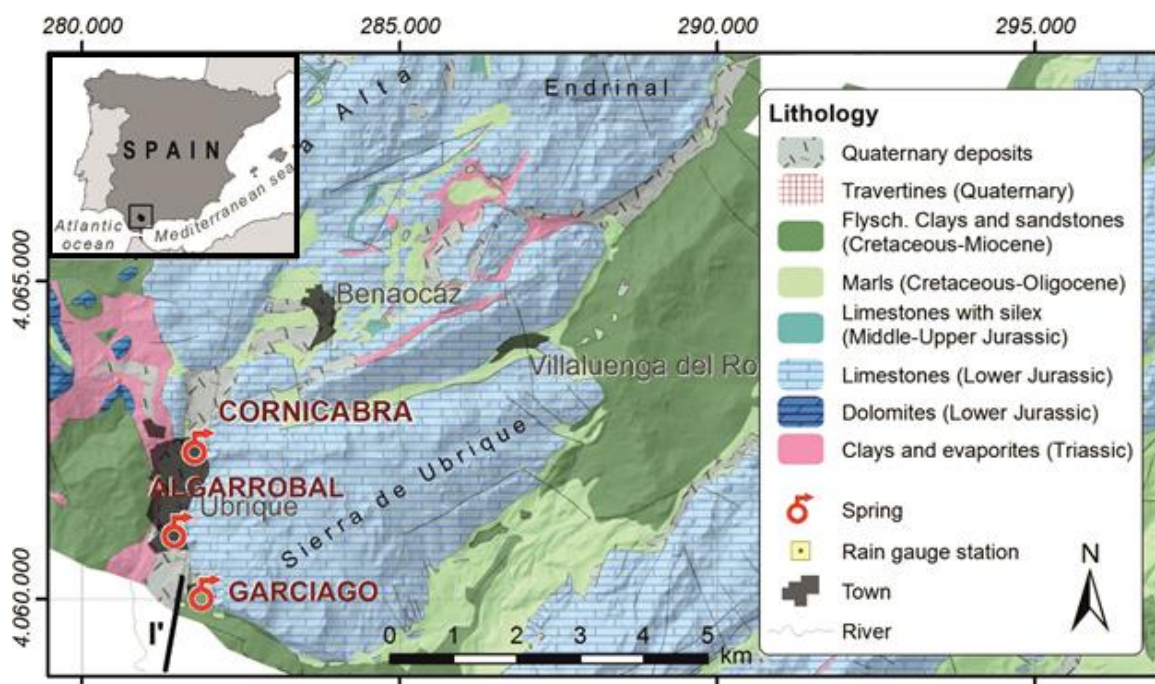


Figure 5.2. Hydrogeological setting of the Sierra de Ubrique aquifer system (modified from Sánchez et al., 2017).

5.2 Water Budget Summary

As described in D2.1 “Preliminary water budget”, two different methods were applied to estimate the different components of the balance equation. In **Eastern Ronda Mountains**, recharge rate was estimated using APLIS method (Andreo et al., 2004; 2008), which finally showed up a mean recharge rate of 56.71 % with a diverse spatial distribution due mainly to altitude differences. Thus, the following equations were applied for water budget calculations:

$$PU = P \times APLIS_{\text{recharge rate}}$$

$$ETR = P - PU$$

Hence, a value of effective rainfall of 17,9 hm³/year was therefore estimated, which shows coherence with previous researches in this area (Tab. 5.1). However, the mean annual discharge through the main discharge points of the system was estimated at 18.9 hm³/year for Barberá (2014) study period and at 15.97 hm³/year for the historical data period (1964/65 - 2009/10).

Table 5.1: Mean renewable resources (hm^3/year) at Merinos-Colorado-Carrasco test site estimated on previous studies (modified from Barberá, 2014).

	Fernández (1980)	IGME (1983)	DPM (1988)	Barberá (2014)
Sierras de Merinos, Colorado y Carrasco	24,3	17,99	17	17,96

In **Sierra de Ubrique** test site, mean effective rainfall data were estimated using climatological and spring flow data from hydrological years 2012/13 to 2014/2015 (Martín-Rodríguez et al., 2016). Furthermore, Thornthwaite (1948) method was applied for ETR estimation with soil water capacity equals to 50 mm. As no storage variations are assumed in historical analyses of water budget, the following equation was applied for water budget calculations:

$$\text{PU} = (\text{P} - \text{ETR})$$

As a result, a mean annual effective rainfall of 31.4 hm^3 (Tab. 5.2) was estimated, and thus, a recharge rate of 75% was obtained. In this case, the mean annual discharge during the study period was 35.1 hm^3 , which supposes a difference of 3.7 hm^3 when compared with estimated mean recharge values.

Table 5.2: Mean recharge values calculated through water budget in soil (Hargreaves equation) with field capacity 50 mm for the 2012/13-2014/15 period (modified from Martín-Rodríguez et al., 2016).

Aquifer	Permeable surface (Km^2)	Total rainfall (PP), effective rainfall (PU) and Real Evapotranspiration (hm^3)											Output (hm^3)			Annual average	Difference	
		2012/13			2013/14			2014/15			Annual average			Hydrological year				
		P	PU	ETR	P	PU	ETR	P	PU	ETR	P	PU	ETR	2012/13	2013/14			2014/15
Ubrique	25,9	56,3	45,1	11,2	39,1	29,2	9,9	29,1	19,8	9,3	41,5	31,4	10,1	52,6	36,4	16,2	35,1	-3,7

The water budget results of both test sites presented in D2.1 are summarized in Table 5.3, where notable differences are observed between them: firstly, the mean annual rainfall is higher in Sierra de Ubrique due to the orographic features and the closeness to the Atlantic sea, and secondly, despite that the total recharge area is higher in Eastern Ronda Mountains, the elevated precipitation and karstification degree in Sierra de Ubrique derives in a higher net infiltration (and consequently, higher recharge rate and renewable resources).

Table 5.3: Summary of main water budget results for different study periods at KARMA project study area (taken from D2.1).

	Merinos-Colorado- Carrasco (Barberá, 2014)	Sierra de Ubrique (Martín-Rodríguez et al., 2016)
<i>Average rainfall</i>	31,7 hm ³ /year	41,5 hm ³ /year
<i>Recharge area</i>	43,2 km ²	25,9 km ²
<i>Net infiltration</i>	18 hm ³ /year	31,4 hm ³ /year
<i>Recharge rate (% Aver. Rainfall)</i>	0,56	0,75
<i>Average temperature</i>	15,3 °C	15,7 °C
<i>ETR</i>	13,71 hm ³ /year	10,1 hm ³ /year
<i>Output</i>	17,0-24,3 hm ³ /year	35,1 hm ³ /year

In order to homogenize the methodology used for the water balance in Spanish KARMA test sites, APLIS method was also applied in Ubrique test site, as shown in D2.2. Hence, the obtained results displayed a slightly lower value for recharge rate (72.84%), and thus, the average renewable resources in this area were estimated to 24.47 hm³/year. However, more accurate APLIS results of an ongoing thesis showed a recharge rate of 64.39% over the carbonate exposures.

5.3 Weakness and Uncertainties of the adopted methods

The two greatest sources of uncertainty in water balance are related to (1) the accuracy of the input and output quantification and (2) the simplifications and assumptions of the calculation methods. In the first case, different factors such as the delineation of the recharge area, the different methods for ETR estimation, the existence of unknown concentrated flow input or temporary outputs as well as the flow measurement methods that might under/overestimate spring discharge during a large period, suppose a continued error in the estimation of the water balance components. In the second case, the simplification that the selected approaches perform on the reality of the systems through the application of equations that represent physical processes.

In the case of **Eastern Ronda Mountains**, the water balance is well established and shows slight differences (less than 10%) between estimated recharge and discharge measured at the springs. Nonetheless, it is important to highlight that the average annual discharge calculated in Barberá (2014) study period may be slightly overrated because the 2009/2010 hydrological year was extremely wet. Even so, APLIS method has proven to be a reliable approach for recharge estimation in this area as it provides recharge rate values that are consistent with the hydrogeological features and karstification degree of the system. In this way, it is possible to confirm that the uncertainty in the estimation of the average renewable resources in the Eastern Ronda Mountains system is very low.

However, the case of **Sierra de Ubrique** test site is slightly more complex due to the specific recharge features. The difference of 3,7 hm³/year when compared with output values (35,1 hm³/year) could be explained as allogenic recharge was not considered for water balance due to the lack of input flow data record during the study period of Martín-Rodríguez et al., (2016). Thus, the application of balance equation using Thornthwaite method in Sierra de Ubrique might be overestimating the mean annual recharge in this area. On the other hand, the application of APLIS method shows approximately 6.93 hm³/year less than the estimated recharge, which can be due to two different causes: (1) the cartography of flow concentration areas that constitute “I” layer on APLIS is not as accurate as it should be for reliable calculations (recharge is underestimated by APLIS); (2) the hydrological years used for water balance in Martín-Rodríguez et al., (2016) were slightly wetter than the average year (period 1984/85 – 2017/18) that was used for the estimation of specific recharge values on APLIS method (recharge is overestimated in Martín-Rodríguez et al., (2016)).

5.4 Validation Tools

Chloride mass-balance method

Chloride is well known as a useful environmental tracer as it presents high solubility and conservative behavior. The chloride mass-balance (CMB) method requires simple data input and allows to directly estimate recharge through the following equation:

$$R = Px \frac{Cl_p^-}{Cl_{Gw}^-}$$

where R is recharge (mm/year); P is rainfall (mm/year); Cl_p⁻ is weighted average chloride concentration in rainfall (mg/l); Cl_{Gw}⁻ and is average chloride concentration in groundwater (mg/l).

The application of this approach at **Eastern Ronda Mountains** has been realized considering the data from Barberá (2014). A rain collector located in Cuevas del Becerro (730 m a.s.l.) was used for precipitation chloride concentration analysis and showed a mean concentration of 1.9 mg/l additionally, the chloride concentrations (weighted the spring discharge) in the main drainage points, Carrizal (12%), Cañamero (81%) and Ventilla (7%) springs, were 9.0 mg/l, 7.1 mg/l and 8.9 mg/l respectively, leading to a value of 7.31 mg/l in groundwater. The mean annual precipitation over this area during the historical period (1964/65 - 2009/10) is 733 mm, thus, the empirical calculation can be expressed as:

$$R = 733 \frac{mm}{yr} \times \frac{1.9 \text{ mg/L}}{7.31 \text{ mg/L}} = \mathbf{190.51 \text{ mm/yr}}$$

The application of this methodology results in a recharge rate of 26% for this area, which substantially differs from that obtained through other approaches.

Moreover, at **Ubrique** test site, during KARMA study period (2021/2022) the chloride concentrations obtained in rainfall samples, as well as Cornicabra (45%), Algarrobal (23%) and Garciago (32%) springs were 1.39, 2.93, 8.37 and 7.56 mg/l respectively, that leads to a value of 5.65 mg/l in groundwater. As the mean annual precipitation in this area, as stated in D2.1, is 1,297 mm, thus, the empirical calculation can be described as:

$$R = 1,297 \frac{mm}{yr} \times \frac{1.39 \text{ mg/L}}{4.98 \text{ mg/L}} = \mathbf{362.01 \text{ mm/yr}}$$

This results in a recharge rate of 28%, that, in the same way as in the previous case, it highly differs from the results obtained by other methods.

Water stable isotopes

The analysis of the spatial variations of water stable isotopes (such as $\delta^{18}O$) provide information about the recharge area given that isotopic values might be correlated to the altitude at which precipitation could have been infiltrated to the aquifer. As the rainfall spatial distribution is normally increasing with altitude, this method might help to verify that the precipitation input values used for the water balance are correct.

The data presented in D2.3 “Stable isotopes” showed that the springs of **Eastern Ronda Mountains**, Cañamero, Carrizal and Ventilla, present a mean $\delta^{18}O$ value of -6.84, -6.52 and -6.42‰ respectively, that according to the equation presented in Figure 7 (also from D2.3) (Barberá, 2014):

$$Altitude = -\frac{\delta^{18}O + 5.3029}{0.0015}$$

Hence, the mean recharge altitudes calculated for these discharge points are 1024.7, 811.4 and 744 m a.s.l.. It is now possible to estimate mean annual precipitation over those altitudes though the application of the equation described in Figure 2 from D2.3 (Barberá, 2014):

$$Precipitation = 0.66 * altitude + 210$$

Thus, it results in 886.3 mm for the recharge area of Cañamero spring, 745.5 for Carrizal and 701 for Ventilla.

In the same way, the analysis of water stable isotopes at **Ubrique** test site springs, Cornicabra, Algarrobal and Garciago, showed mean $\delta^{18}O$ values of -5.91, -5.58 and -5.39‰ respectively. The equation that establishes the relationship between recharge altitude and mean $\delta^{18}O$ values was as well described by Sánchez et al., (2018):

$$Altitude: -328.6 * \delta^{18}O - 810$$

Therefore, the mean recharge altitudes estimated for Ubrique test site discharge points are 1132, 1023 and 961 m a.s.l.. The relationship between annual rainfall and altitude, as described by Sánchez and Andreo (2013), can be expressed as:

$$Precipitation = 1.14 * altitude + 590.27$$

Thus, it results in 1880 mm for the recharge area of Cornicabra spring, 1756.5 for Algarrobal and 1685.8 for Garciago.

5.5 Discussion and Conclusions

The wrong estimation of the recharge area directly affects to the calculation of the total input by rainfall, furthermore, other uncertainty sources might be linked to subjectivity, such as the case of APLIS “I” layer, where the personal criteria for classifying fast infiltration landforms may depend on the user. In the same way, the over/underestimation of spring discharge by the measurement equipment used during an investigation can lead to potential biases of data recorded by continuous measurement devices and thus, introducing a great uncertainty in the total output data. Both problems are avoided in Spanish KARMA test sites due to the fact that the aquifers are certainly small, its limits are well defined because of tectonic features and the main drainage points are well known and monitored.

Additionally, in order to verify the obtained results and test the uncertainty of the specific approaches, validation tools such as chloride mass balance are applied, which constitute a reliable method that have been worldwide applied. However, the geogenic origin of chloride in Spanish KARMA test sites (due to the existence of Triassic evaporites in the lower levels of the aquifer) make the application of this method result in recharge rate values much below the real ones. On the other hand, the use of stable water isotopes, which have been well studied at both study areas, display results that are much closer to those measured by weather stations, although they tend to slightly overestimate the precipitation. Nevertheless, this difference might be due to the location of the weather stations in lower altitudes so that the isotopic analyses allow to correct the precipitation data series in some cases.

In spite of the different sources of uncertainty, there is no great disproportion between outputs and inputs in the water balances calculated at the Spanish KARMA test sites mainly due to the existence of previous researches in the study areas (Barberá, 2014; Martín-Rodríguez et al., 2016, Sánchez and Andreo, 2013; Sánchez et al., 2018) that provide a good knowledge of the systems. Furthermore, the application of different methodologies and validation tools allowed to test the reliability and accuracy of the input component estimation methods and results obtained in the water balance through different approaches. Hence, the generated information and knowledge are of great importance for the management of the available groundwater resources in a context of climate change, since both test sites are used for drinking water supply of small populations in mountainous areas of Southern Spain.

5.6 References

- Andreo, B., Vías, J., López-Geta, J.A., Carrasco, F., Durán, J.J. and Jiménez, P. (2004). *Propuesta metodológica para la estimación de la recarga en acuíferos carbonáticos*. Boletín Geológico y Minero 115 (2), 177-186.
- Andreo, B., Vías, J.M., Durán, J.J., Jiménez, P., López-Geta, J.A. and Carrasco, F. (2008). *Methodology for groundwater recharge assessment in carbonate aquifers: application to pilot sites in southern Spain*. Hydrogeology Journal 16 (5), 911-925.
- Barberá, J.A. and Andreo, B. (2012). *Functioning of a karst aquifer from S Spain under highly variable climate conditions, deduced from hydrochemical records*. Environ Earth Sci 65, 2337–2349.
- Barberá, J.A. (2014). *Investigaciones hidrogeológicas en los acuíferos carbonáticos de la Serranía Oriental de Ronda (Málaga)*. PhD Thesis. University of Málaga, Spain. 591 p.
- Marín, A.I., Martín Rodríguez, J.F., Barberá, J.A. Fernández-Ortega, J., Mudarra, M., Sánchez, D., and Andreo, B. (2021). *Groundwater vulnerability to pollution in karst aquifers, considering key challenges and considerations: application to the Ubrique springs in southern Spain*. Hydrogeol J 29, 379–396.
- Martín-Algarra, M. (1987). *Evolución geológica alpina del contacto entre las Zonas Internas y Externas de la Cordillera Bética*. PhD Thesis, University of Granada, Spain. 1171 p.
- Martín-Rodríguez, J.F., Sánchez-García, D., Mudarra-Martínez, M., Andreo-Navarro, B., López-Rodríguez, M., and Navas-Gutiérrez, M.R. (2016). *Evaluación de recursos hídricos y balance hidrogeológico en acuíferos kársticos de montaña. Caso de la Sierra de Grazalema (Cádiz, España)*. Book chapter on *Las aguas subterráneas y la planificación hidrológica*, 163-170. Spanish-Portuguese Congress. IAH Spanish Chapter. Madrid (Spain), November 2016.

Sánchez, D. and Andreo, B. (2013). *Caracterización hidrogeológica y evaluación de los recursos hídricos de la Sierra de Grazalema (Cádiz) para su potencial implementación como reserva estratégica de cabecera de la Demarcación Hidrográfica del Guadalete-Barbate*. Informe de resultados del periodo de control noviembre 2012-noviembre 2013. Junta de Andalucía

Sánchez, D., Barberá, J.A., Mudarra, M., Andreo, B. and Martín, J.F. (2018). *Hydrochemical and isotopic characterization of carbonate aquifers under natural flow conditions, Sierra Grazalema Natural Park, southern Spain*. Geological Society, London, Special Publications, 466, 275-293

Thornthwaite, C. W. (1948). *An approach toward rational classification of climate*. Geographical Review 38 (1), 55-94.

6 The Lez Karst Catchment (case study France)

6.1 Water Budget Results Summary

The water budget on the Lez catchment was estimated using water balance and GIS methods (APLIS, Andreo et al. (2008), Marín (2009)). The water balance method gives an idea of the volume of water that is stored or lost each year with the following formula:

$$\Delta S = P - ET - Q$$

With ΔS the variation in stock (mm), P the precipitation on the catchment (mm), ET the evapotranspiration on the catchment (mm) and Q the water level leaving the catchment, by flow or pumping (mm). The APLIS method is a multi-criteria method for estimating the recharge rate in a catchment. It is based on the spatial analysis of different components of a catchment: altitude, slope, lithology, infiltration and pedology.

Table 6.1: Estimation of the annual recharge on the Lez catchment according to (i) a water balance method and (ii) APLIS method.

Year	Precipitation (mm)	Annual recharge (hm ³ /year)	
		APLIS method	Water balance method
Dry (1952-1953)	438	28.3	10.9
Intermediate (1955-1956)	916	59.5	58.3
Wet (1995-1996)	1763	114.5	161.8

The annual recharge for an intermediate year is estimated at 59.5 hm³ with the APLIS method and at 58.3 hm³ with the water balance method. These results are very similar and consistent with the mean annual volume that leaves the system (natural flow at the spring and pumping) estimated at 58.5 hm³. The annual recharge for a dry year is estimated to be lower with the water balance method (10.9 hm³ against 28.3 hm³ with APLIS), which may be related to the evapotranspiration processes that are not considered in the APLIS method. The annual recharge for a wet year is estimated to be higher with the water balance method (161.8 hm³ against 114.5 hm³ with APLIS), which is likely due to the run-off volume that is not considered in the water balance method but should be withdrawn to get the effective recharge.

6.2 Weakness and uncertainties of the adopted methods

6.2.1 Water Balance Method

The water balance method presents uncertainties on the input data (precipitation and evapotranspiration) and the delineation of the catchment. Precipitation is considered to be relevant for the Lez catchment. The precipitation time series is derived from 4 meteorological stations spread over the catchment area (Prades-le-Lez, Sauteyrargues, Saint-Martin-de-Londres, Valfaunès). The time

series was interpolated with the Thiessen polygon method to obtain an equivalent precipitation over the catchment area.

On the other hand, there are uncertainties on evapotranspiration because it is generally derived from other meteorological variables (mainly temperature). We carried out a sensitivity analysis on potential evapotranspiration at the scale of the Lez catchment, comparing 10 methods of potential evapotranspiration with the actual evapotranspiration measured at Puéchabon. The Puéchabon platform is an experimental station set up in a holm oak forest. It has a flux tower that measures a certain number of climatic parameters and parameters related to ecosystem functioning. It is located approximately 22 km west of the Prades-le-Lez weather station where the geology corresponds to Jurassic limestones covered by holm oak forest, these characteristics being similar to the one observed over most of the Lez spring recharge catchment. The actual evapotranspiration (AET) is estimated from the latent heat energy (LE) flux data measured at the station. The 10 potential evapotranspiration methods considered are :

- T-PEN-full, corresponding to the daily PET estimated by the Penman-Monteith formula (Allen et al., 1998) ;
- T-PEN, corresponding to the daily PET estimated by the Penman-Monteith formula and only with the temperature (Allen et al., 1998) ;
- TH, corresponding to the daily PET estimated by the daily Thornthwaite formula (Pereira and Pruitt, 2004) ;
- TU, corresponding to the daily PET estimated by the Turc formula (Turc, 1961) ;
- HA, corresponding to the daily PET estimated by the Hargreaves formula with global radiation (Hargreaves and Samani, 1985) ;
- T-HA, corresponding to the daily PET estimated by the Hargreaves formula with the temperature (Hargreaves, 1975) ;
- OU, corresponding to the daily PET estimated by the formula of Oudin et al. (2005) ;
- PT, corresponding to the daily PET estimated by the formula of Priestley (1972) ;
- MH, corresponding to the daily PET estimated by the formula of Makkink (1957) with the correction of Hansen (1984);
- GR, corresponds to the daily PET estimated by the Penman-Monteith formula at grid points.

The comparison of the different methods for estimating the daily PET with the AET measured at Puéchabon was carried out over the period 1992-01-01 to 2018-12-31. All methods significantly overestimate evapotranspiration, with up to 300% deviation from the AET measured at Puéchabon. The MH and OU methods give the closest estimates to the AET with mean annual deviations of 103% and 101% (Figure 6.1).

The significant difference between the PET calculated by the different methods and the AET is not surprising, given that the PET methods generally calculate the maximum evapotranspiration that could be observed if conditions allowed, which is very rarely the case. Moreover, some methods are developed from observations and measurements on a grass plot, which is a very different environment from the holm oak forest found at the Puéchabon experimental site. PET methods are generally developed and used in agriculture where saturation conditions can be maintained.

These results highlight the low relevance of PET methods for approaching AET at the scale of a catchment area, where the conditions (water volume, energy input) are absolutely different from those found at the scale of a crop plot.

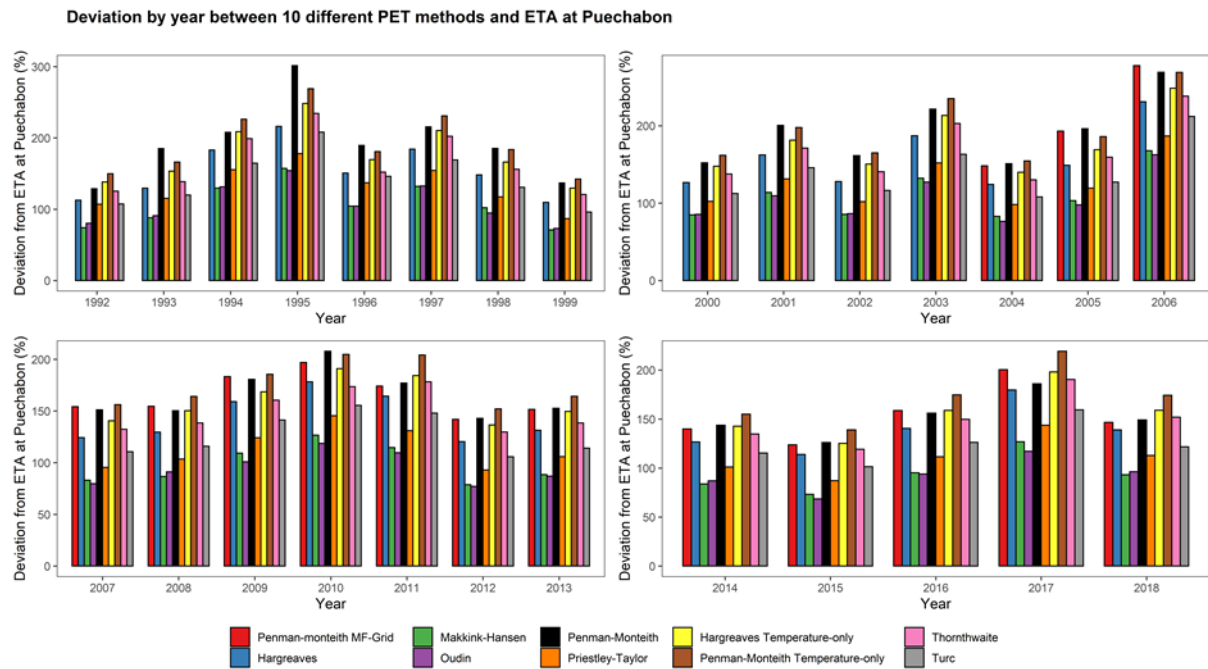


Figure 6.1. Deviation by hydrological year between 10 different PET methods and actual evapotranspiration at Puéchabon

It therefore seems appropriate to use the AET data measured at Puéchabon, which are more representative of the vegetation and evapotranspiration that could be found in the catchment area, to carry out the water balance of the Lez.

To better explore the uncertainties related to evapotranspiration, we used a soil water reserve (SWR) model to estimate the AET from the input rainfall and PET data (Figure 9). The model consists of filling a reservoir corresponding to the soil water reserve from the difference between precipitation and PET, and then determining the AET by stating:

- If, on $d+1$, the level (E) of the SWR is higher than E_{min} , then the AET on day d is equal to the PET;
- If, on $d+1$, the level (E) of the SWR equal E_{min} , then the AET on day d is equal to the sum of precipitation (P) and volume contained in the SWR (E) minus the recharge (R), on day d .

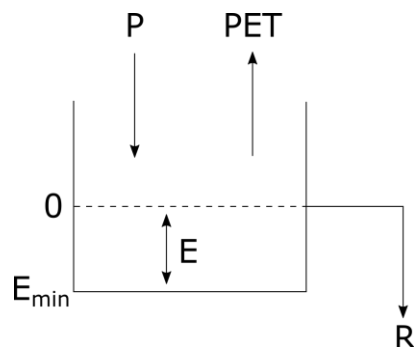


Figure 6.2. Model Structure

The model includes two parameters to be calibrated (Figure 6.2):

- k (1/day), corresponding to the specific discharge coefficient of the SWR, i.e. the daily fraction participating in the recharge (R) corresponding to kE ;
- E_{min} , corresponding to the minimum level of the SWR.

The model was tested with 9 methods of PET (grid PET was not considered as there is less data available) and the results were compared with the AET measured at Puéchabon by measuring the percentage deviation. As the daily and monthly estimates were largely erroneous, the comparison was made with the annual balances, where the complete emptying of the reservoir during low water periods compensates for the overestimation of the ET (Figure 6.3). The results show that the annual scale simulation of AET is correct (average interannual deviation less than 10%) and that the input PET model has little influence on the results (deviation from 7.6% to 9.23%).

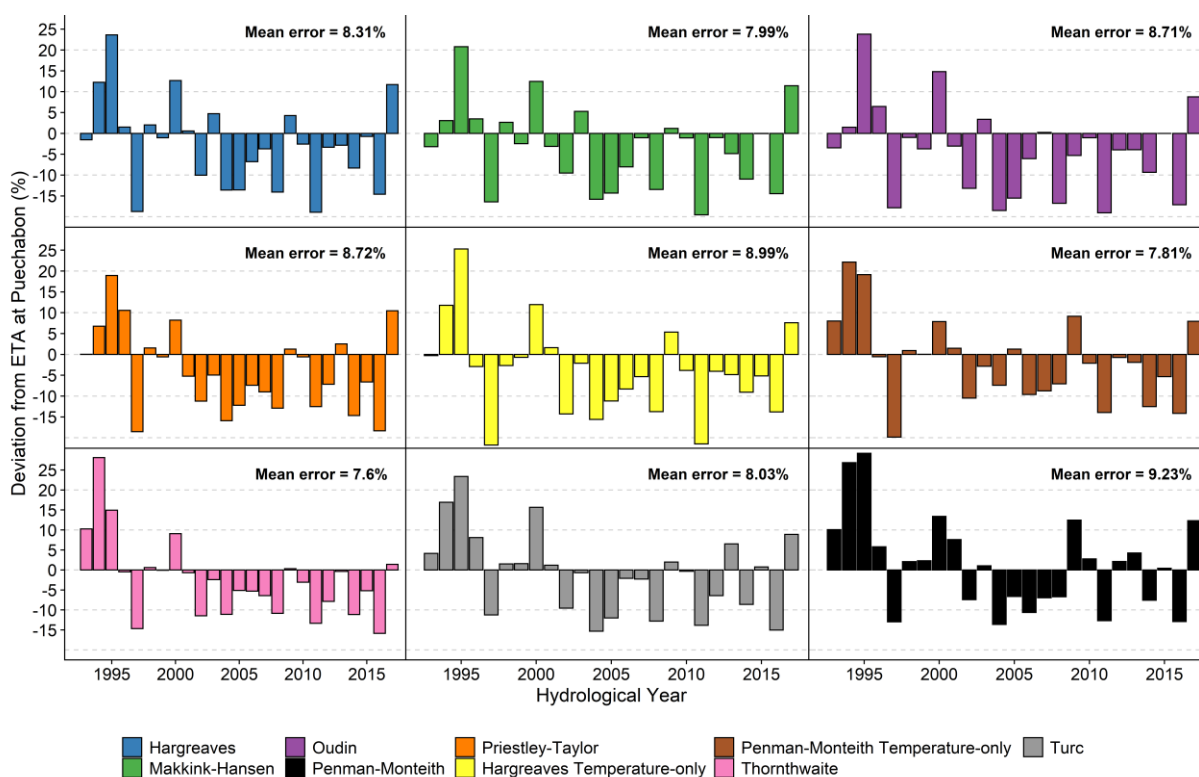


Figure 6.3: Annual deviation (%) between evapotranspiration calculated with the model against actual evapotranspiration measured at Puéchabon.

6.2.2 APLIS Method

The resolution of the DEM (75m) may induce some errors regarding the influence of localized recharge points (sinkholes). Indeed, as they are about 2-10 m diameter, they do not necessarily appear on the karst features raster file. The poor resolution of the soil layer (1/1000000) with a large majority of leptosols may induce a slightly overestimation of the recharge rate, as the leptosols are very shallow and have close to zero ability to hold water.

The method seems to provide an accurate estimation of the recharge at the scale of the Lez spring catchment, but we feel that the results could be improved by considering the land cover:

- The urban areas (approximately 20 km²) where the infiltration is insignificant.

- The vegetation, which intercepts a part of the precipitation and release water from the soil and vadose zone to the atmosphere via the process of transpiration. This volume may be significant, especially in summer where the demand from the vegetation is high and the evapotranspiration is larger than the precipitation.

6.2.3 Delineation of the Catchment

There are generally uncertainties regarding the boundaries of the recharge area. The Lez catchment area has been the subject of numerous tracer tests (Figure 6.4). Several tracer tests have been carried out since 1960 but their results are questionable due to the detection methods used at the time (active carbon and visual detection). Several tests were subsequently carried out (Clauzon et al., 2020; Dausse, 2015; Jourde et al., 2011; Léonardi et al., 2013) to reduce the existing uncertainties on the initial knowledge. The details of the different tracer tests can be found in Deliverable D2.4. These tracer tests allow a precise delimitation of the recharge area of the Lez spring and characterize the nature of the underground flows.

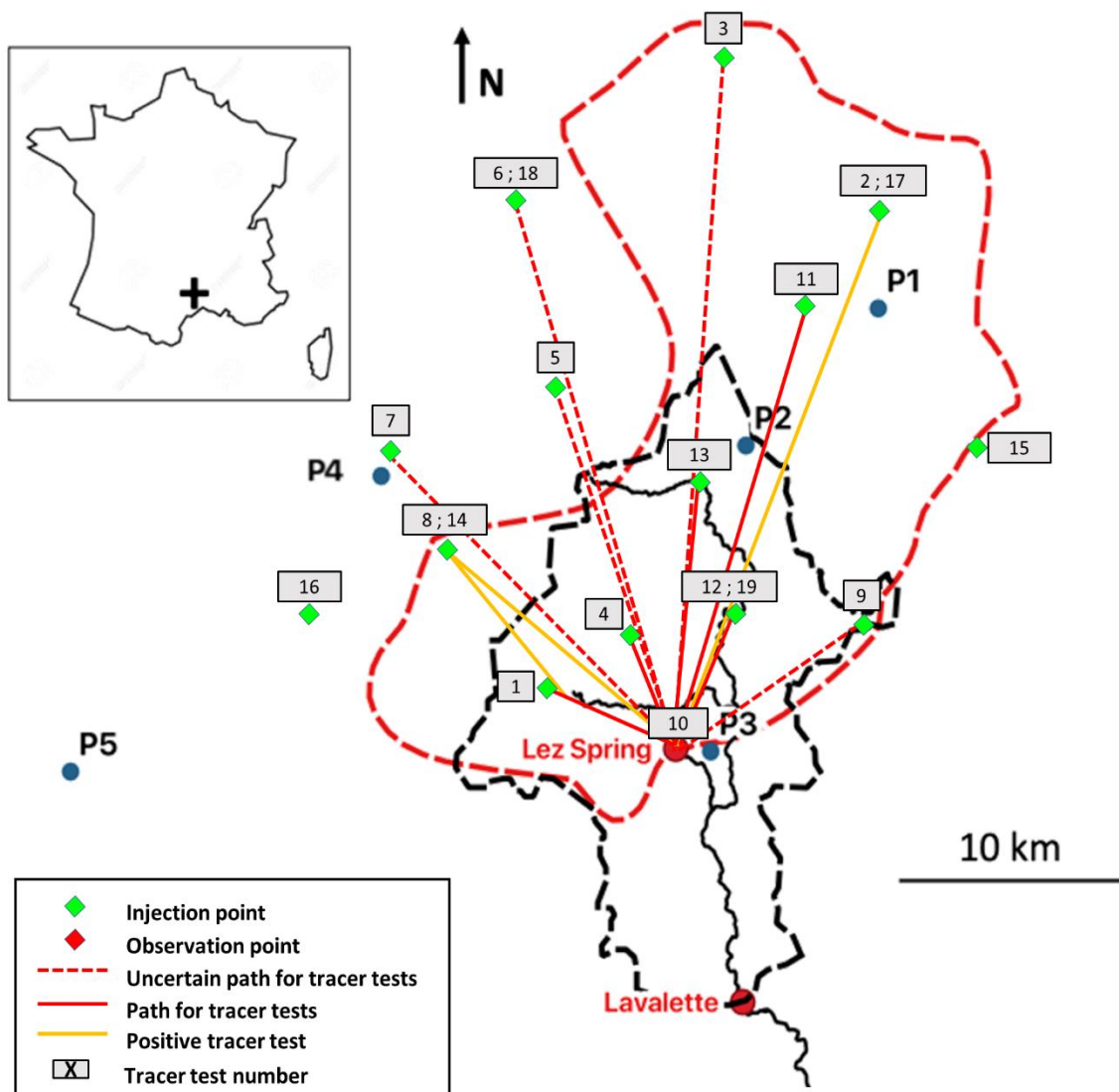


Figure 6.4: Pattern of artificial tracer tests, boundaries (red dashed line) of the Lez spring hydrogeological basin under natural flow regime, and limits (black dashed line) of the Lez River hydrological catchment at Lavalette (modified after Léonardi et al. (2013)).

6.3 Validation Tools

6.3.1 Modelling

Deliverable D4.2 presents a reservoir modelling approach applied to the Lez catchment. The spring flow and piezometric level were simulated using meteorological inputs (precipitation and evapotranspiration). The validation of the results obtained with the APLIS and water balance methods could only be done on an intermediate year because the modelling was performed for the years 2008-2018.

The model recharge estimated on the Lez system (59.8 hm³) is very close to the recharge estimated with the APLIS method (59.5 hm³) and water balance method (58.3 hm³).

6.3.2 APLIS recharge area

The results obtained with the APLIS method (presented in Deliverable D2.2) are consistent with our actual knowledge of the system, especially regarding the main recharge area of the catchment (estimated to 120-150 km² in previous studies, Fleury et al. (2009)):

- We can see on the APLIS recharge map that the main Jurassic limestone outcrops (west and north-west parts of the basin) mostly contribute to the recharge of the aquifer, with a mean recharge rate of 47% for an area of 80 km². The recharge contribution from this area is about 60% of the overall recharge on the catchment (Figure 6.5)
- Other limestone outcrops among the basin, as well as geological features (major faults and sinkholes), also contributes well to the recharge.

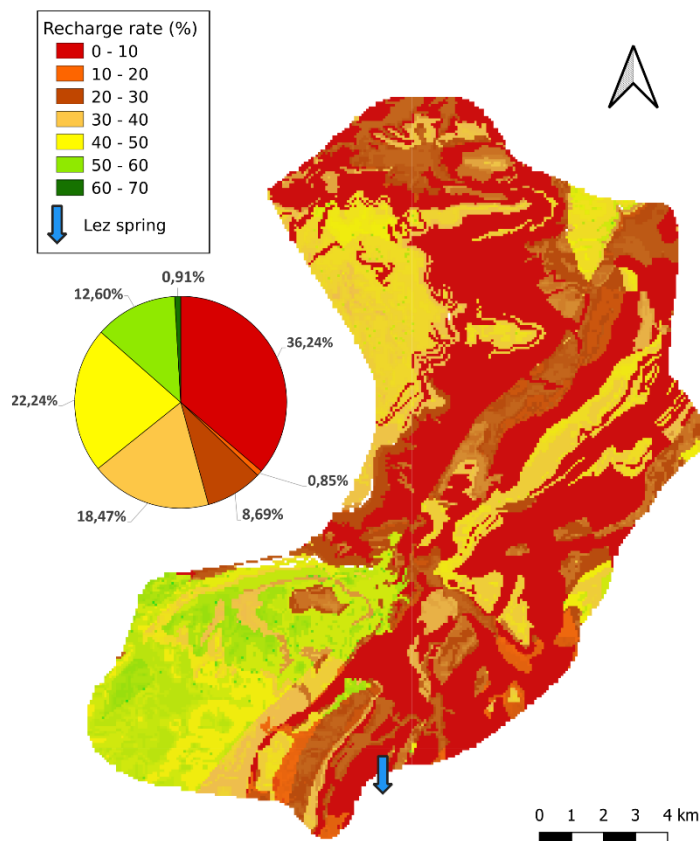


Figure 6.5: Recharge rate (% of total precipitation) on the Lez catchment.

6.4 Discussion and Conclusion

On the Lez catchment, the water budget has been initially calculated with water balance and APLIS methods. These two different approaches gave fairly close results, especially for the intermediate water periods. Several uncertainties have to be considered when assessing the results of the water budget:

- The evapotranspiration is approximated by an actual evapotranspiration measured at 22 km from the catchment, as it is considered to be the closest to reality. The comparison of several potential evapotranspiration has shown significant uncertainties with respect to the actual evapotranspiration (up to 300%). However, the use of a soil water reserve model can give good results on an annual scale using potential evapotranspiration.
- The uncertainty on precipitation is minimised by using four meteorological stations spread over the Lez catchment. The precipitation time series was interpolated using the Thiessen polygon method, allowing for an equivalent precipitation over the entire catchment area.
- The delineation of the catchment area was initially proposed on the basis of old tracer tests (active carbon and visual detection) and has been reinforced since 2010 by a tracer test campaign to reduce the uncertainty of the initial methods used.
- The APLIS method also presents uncertainties in relation to the input data, which will be more or less important depending on the resolution and quality of the information.
- The APLIS method does not take into account certain aspects of land use: (i) urban areas where infiltration is negligible, and (ii) vegetation, which intercepts part of the precipitation and releases part through transpiration.

The reservoir modelling confirmed the mass balances estimated with the water balance and multi-criteria mapping methods. The APLIS recharge area appears to be consistent with known limestone karstification, giving a preferential recharge area of about 120-150 km².

6.5 References

Allen, R.G., Pereira, L.S., Raes, D., Smith, M., FAO (Eds.), 1998. Crop evapotranspiration: Guidelines for computing crop water requirements, FAO irrigation and drainage paper. Food and Agriculture Organization of the United Nations, Rome.

Andreo, B., Vías, J., Durán, J.J., Jiménez, P., López-Geta, J.A., Carrasco, F., 2008. Methodology for groundwater recharge assessment in carbonate aquifers: Application to pilot sites in southern Spain. *Hydrogeol J* 16, 911–925. <https://doi.org/10.1007/s10040-008-0274-5>

Clauzon, V., Mayolle, S., Leonardi, V., Brunet, P., Soliva, R., Marchand, P., Massonnat, G., Rolando, J.-P., Pistre, S., 2020. Fault zones in limestones: Impact on karstogenesis and groundwater flow (Lez aquifer, southern France). *Hydrogeol J* 28, 2387–2408. <https://doi.org/10.1007/s10040-020-02189-9>

Dausse, A., 2015. Facteurs d'échelle dans la hiérarchisation des écoulements au sein d'un aquifère karstique. (PhD thesis). Montpellier.

Fleury, P., Ladouche, B., Conroux, Y., Jourde, H., Dörfliger, N., 2009. Modelling the hydrologic functions of a karst aquifer under active water management The Lez spring. *Journal of Hydrology* 365, 235–243. <https://doi.org/10.1016/j.jhydrol.2008.11.037>

Hansen, S., 1984. Estimation of Potential and Actual Evapotranspiration. *Hydrology Research* 15, 205–212. <https://doi.org/10.2166/nh.1984.0017>

Hargreaves, G.H., 1975. Moisture Availability and Crop Production. Transactions of the ASAE 18, 0980–0984. <https://doi.org/10.13031/2013.36722>

Hargreaves, G.H., Samani, Z.A., 1985. Reference Crop Evapotranspiration from Temperature. Applied Engineering in Agriculture 1, 96–99. <https://doi.org/10.13031/2013.26773>

Jourde, H., Dörflinger, N., Maréchal, J.-C., Batiot-Guilhe, C., Bouvier, C., Courrioux, G., Desprats, J.F., Fullgraf, T., Ladouche, B., Leonardi, V., Malaterre, P.O., Prié, V., Seidel, J.-L., 2011. Projet gestion multi-usages de l'hydrosystème karstique du Lez - Synthèse des connaissances récentes et passées ({{BRGM}} No. RP-60041-FR).

Léonardi, V., Jourde, H., Dausse, A., Dörflinger, N., BRUNET, P., Maréchal, J.-C., 2013. Apport de nouveaux traçages et forages à la connaissance hydrogéologique de l'aquifère karstique du Lez. KARSTOLOGIA 7–14.

Makkink, G., 1957. Testing the Penman formula by means of lysimeters. Journal of the Institution of Water Engineers 11.

Marín, A.I., 2009. The Geographic Information Systems applied to the evaluation of groundwater resources and to the vulnerability to the contamination of carbonate aquifers: The case example of the Alta Cadena aquifer (Malaga province) (PhD thesis). Malaga, Spain.

Oudin, L., Hervieu, F., Michel, C., Perrin, C., Andréassian, V., Anctil, F., Loumagne, C., 2005. Which potential evapotranspiration input for a lumped rainfallrunoff model?: Part 2 a simple and efficient potential evapotranspiration model for rainfallrunoff modelling. Journal of Hydrology 303, 290–306. <https://doi.org/10.1016/j.jhydrol.2004.08.026>

Pereira, A.R., Pruitt, W.O., 2004. Adaptation of the Thornthwaite scheme for estimating daily reference evapotranspiration. Agricultural Water Management 66, 251–257. <https://doi.org/10.1016/j.agwat.2003.11.003>

Priestley, B., 1972. On the Assessment of Surface Heat Flux and Evaporation Using Large-Scale Parameters 12.

Turc, L., 1961. Evaluation des besoins en eau d'irrigation, évapo-transpiration potentielle. Annales agronomiques 12, 13–49.

7 Conclusions

The comparison of water budget obtained in each study area by the national research units clearly allow to reach the following common findings:

- Uncertainties in field data represent a common risk, to be tackle by intense monitoring of recharge factors (as precipitation and temperature), but complete data series of discharge are mandatory to have a correct reference point for any water budget method; long-period recording is recommended to build a successful budget and to use modeling to validate the budget calculations;
- Distributed recharge evaluation of the study areas is recommended but not easy to obtain from climate data; the adoption of the APLIS method based on geological and morphological information results to be a valid tool for recharge calculation in all study areas, even though with clear method limitations;
- The definition of the extension of the recharge area and of its limits is frequently source of uncertainties, where groundwater divides are not sharp, as happen in karst aquifers, and the role of stratigraphic and mainly tectonic limits can be no very clear;
- Field tool as tracer tests, but also chemical-physical parameter monitoring and stable isotope evaluation, result to be very useful for direct validation of the water budget, both in terms to confirm/modify the conceptual model of groundwater flow, and to quantify the recharge rate and their mechanisms;
- Modeling tools have been applied successful mainly where long time-series and detailed conceptual model have been previously developed;
- In general, a valuable water budget with limited (and locally very limited) uncertainties have been carried out in each study area;
- The aquifer extension and the observation scale (regional to local one) have consequences in the uncertainties too.

Final remarks will be obtained during the following final phase of the project, by the D2.8 (Water Availability), where the values of the recharge evaluated with time, will be compared with water abstraction for human uses and, possibly, with natural trend in groundwater recharge (to be related to climate change effects), to finally assess the real water availability in each study area.

Possible and expected common results in availability trends will be discussed, also in terms of sustainability of human pressures for the next future.